SELECTION OF AN OPTIMAL, NON-DESTRUCTIVE INSPECTION TECHNIQUE FOR WELDED COMPONENTS

MOHAMED KHALIFA

Selection of an Optimal, Non-Destructive Inspection Technique for Welded Components

A THESIS

Submitted to the School of Graduate Studies in partial fulfillment

of the requirements for the degree of Master of Engineering

BY

Mohamed Khalifa, B.Sc. (Eng)

Faculty of Engineering and Applied Science

Memorial University of Newfoundland

(2009)

St. John's Newfoundland Canada

Abstract

The objective of this work is to select an optimum Non-Destructive Inspection (NDI) technique and its associated inspection interval for welded components subjected to cyclic loading.

The objective function (total cost) is formulated as a function of the decision variables (controllable) and condition of the inspected asset (uncontrollable). Total cost consists of inspections cost and repairs cost over the lifetime and risk of failure as a result of the failure to detect a growing crack before it reaches a critical size. The decision variables are the reliability of the NDI technique and the inspection interval. Two main parameters are used to quantify the reliability of the NDI techniques. These are the Probability of Detection function (POD) and the Probability of False Calls, (PFC). Condition of the inspected asset is represented by the probability of the presence of a crack in the inspected asset at inspection time and the expected time to failure. The objective function is minimized for different NDI techniques subject to a safety constraint: that the probability of failure as a result of failure to detect a growing crack before it reaches the critical size does not exceed a predefined limit. The minimum values of the objective functions for all candidate NDI techniques are compared to determine the optimal NDI technique and its associated inspection interval.

Acknowledgements

First of all, never enough thanks are to the Merciful Allah, who gives me everything I have. I would like to express my gratitude and appreciation to my supervisors, Dr. M. Haddara and Dr. F. Khan for the proper suggestion and planning of the research project, encouragement, valuable comments, continuous kind support, their guidance throughout my thesis and never accepting less than my best efforts.

I would also like to convey thanks to Faculty of Engineering and Applied Science and the School of Graduate Studies.

I would also like to thank the library staff at MUN for their tireless efforts.

Finally, I take this opportunity to express my thanks and gratitude to my wife and my family members; for their understanding and endless love, through the duration of my study and throughout my entire life.

Contents

List of Figures

List of Tables

List of Symbols

NDI	Non-Destructive Inspection
a	Crack size
POD	Probability of Detection
PFC	Probability of False Calls
H	Probability of presence a crack
f(a)	Probability density function of the crack size
$\Delta\sigma$	Applied stress range
$\Delta\sigma_{eff}$	Effective stress range
f	Stress frequency
a_o	Initial crack size
a_{cr}	Critical crack size
C and m	Material parameters for fatigue crack growth
t_{cr}	Critical time to failure
t_{int}	Inspection interval
t	Time
t_1	Time to the first inspection
$E[P_f]$	Expected probability of failure
$P_{f,accept}$	Acceptable probability of failure
OF	Objective function
JR	Justifiable repair
FR	False repair
$f(a_f)$	Probability density function of the cracks size indicated as false calls
A_i	Probability of acceptance of crack with size ai

E[n]	Expected number of inspections during the lifetime
N_1	Number of simulations at which the first inspection time, t1, is less than or equal the critical time
N_2	Number of simulations at which the first inspection time is more than the critical time
N	Total number of simulations
n_j	Number of inspections in simulation number "j"
K_I	Cost of one inspection
K_F	Cost of failure
K_R	Cost of one repair
F(a)	Geometry function
Δk	Stress intensity range factor
k	Stress intensity factor

Chapter 1

Introduction

Inspections during the lifetime of a structure or a piece of equipment are carried out to make sure that the structure or the equipment is running according to the design specifications and to guarantee a specified acceptable level of safety throughout the lifetime of the asset.

Even with the highest quality of materials and workmanship, the occurrence of some form of discontinuity or flaw during manufacture is inevitable. Flaws can be categorized into pre-service and in-service flaws depending on whether they originated during manufacture or in-service. The manufacturing quality can be achieved using well established engineering practices. In-service, the material is subjected to degradation

caused by different mechanisms which may result in crack initiation and propagation. Hence, in-service inspection is required at regular intervals. Inspection results can be used in performing maintenance tasks to mitigate risk of failure. These inspections are usually carried out using one of the well established Non Destructive Inspection (NDI) techniques.

Fatigue cracks are very common in welded components. Despite the best care taken during design, fabrication and inspection, many of the welded components fail as a result of fatigue cracks initiated at the welding zone, especially at welding flaws. These flaws include but not limited to the existence of cavities, porosities, slag inclusions and poor fusion.

1.1 Objective

An optimal inspection plan provides inspections at the right location, at the right time using the right tool and at the lowest cost without compromising the required safety level. The objective of this thesis is to select an optimum Non-Destructive Inspection (NDI) technique and its associated inspection interval for in-service inspection of welded components.

1.2 Literature Review

The available literatures which are focusing on optimization of the inspection planning are mainly looking for answering three questions:

1- Which equipment or component in equipment or structure is more critical and need to be inspected more frequently (i.e prioritization of component inspections).

2- When the inspection should be scheduled (i.e, selection the optimum inspection interval).

3- What inspection method or technique should be used (i.e. selecting an optimum inspection technique).

A number of papers in the literature discuss the problem of prioritization of component inspections and selecting an optimum inspection interval but few address the problem of selecting an optimum inspection technique.

Review of Component Inspections Prioritization / Selecting an Optimum Inspection Interval

In 1991, the American Society of Mechanical Engineers (ASME) developed a risk based inspection. ASME risk based inspection approach consisted of four steps: definition of the system, a qualitative risk assessment, a quantitative risk assessment, and development of inspection program

In May 1993, the American Petroleum Institute (API) initiated a risk based inspection (RBI) project aimed at building an RBI methodology that uses risk as a base for prioritizing and managing inspection programs. The API RBI approach is carried out based on two levels of analysis: qualitative analysis and semi-quantitative analysis. The qualitative approach uses engineering experience and judgment as the bases for the risk analysis. Therefore, the accuracy of the results in the qualitative RBI approach depends totally on the analyst's experience and background. The semi-quantitative approach combines the speed of the qualitative approach and the accuracy of the quantitative

approach. The data required for the semi-quantitative approaches are mostly like the ones required for quantitative approaches with less details. The API approach ranks the equipments or the components through a 5x5 matrix of likelihood and consequence. The ranking gives classification of the equipments or the component based on level of the risk (e.g. high, medium, low). The developed RBI methodology was published in 2000 as API 581.

Veswly, Belhadje, and Renzoes (1994) presented a probabilistic risk assessment for maintenance prioritization applications based on risk level.

Nessim and Stephens (1995) presented a risk based methodology for selecting the optimum maintenance (i.e. repair and inspection) interval for hydrocarbon pipelines segments.

Vaurio (1995) presented a general procedure to optimize inspection and maintenance intervals of safety related systems and components. Optimization was done based on minimizing the cost under the condition that risk remains below a set criterion.

Balkey, Art and Bosnk (1998) developed a risk based ranking methodology that includes probabilistic risk assessment (PRA) method. The developed methodology integrates nondestructive examination data, failure data, structural reliability and probabilistic risk assessment.

Hagemeijer and Kerkveld (1998) developed a risk based methodology which aims at optimizing the inspection and maintenance based on minimizing the risk.

Harnly (1998) developed a risk ranked inspection recommendation procedure to prioritize repairs identified during equipment inspection.

Apeland and Aven (2000) developed a risk based maintenance optimization approach. The optimal strategies can be determined by evaluating the relationship between the benefits associated with each maintenance alternative and its cost.

Nessim, Stephens, and Zimmerman (2000) presented a quantitative risk based integrity model for maintenance planning for offshore pipelines. Benefits associated with different maintenance alternatives are quantified by calculating their impact on the risk of failure.

Dey (2001) presented a methodology to identify the right pipeline for inspection and maintenance policy; reduces the cost of inspecting and maintaining petroleum pipelines; reduces the time spent on inspection; and suggests efficient design and operation philosophies, construction methodology and logical insurance plans.

Kallen (2002) developed a probabilistic risk based inspection methodology to develop optimal safety inspection plans. Cost functions associated with the deterioration due to corrosion are developed. The corrosion deterioration was modeled using gamma stochastic deterioration process.

Chung et al (2003) proposed a reliability-based optimal inspection scheduling. The objective function includes the total expected cost of inspection, repair, and failure formulated on the basis of an event tree framework and appropriate constraints in inspection intervals and minimum (target) structural reliability. The proposed reliability-

based optimal inspection scheduling gives an optimal inspection-scheduling plan for a specified fatigue details (fracture-critical details).

Khan and Haddara (2003) presented a risk based maintenance methodology for designing an optimum inspection and maintenance programs for heating, ventilation and air-conditioning (HAVAC) systems.

Fujiyama et al (2004) developed a risk based maintenance (RBM) system for determining optimum maintenance and inspection plan for steam turbine plants. The developed risk based maintenance system makes use of the field failure and inspection database accumulated over 30 years.

Kallen and Noortwijk (2004) developed a risk inspection technique used in optimal inspection and replacement decisions for multiple failure modes. The deterioration model is presented along with the cost functions. The cost functions were extended to include multiple failure modes.

Khan and Haddara (2004a) proposed a risk based maintenance (RBM) methodology to answer two questions: the maintenance program should be scheduled for which equipment? and when the maintenance should be scheduled?

Khan and Haddara (2004b) developed a comprehensive and quantitative methodology for maintenance planning based on risk. This methodology is developed to obtain an optimum maintenance schedule that minimizes the probability of failure and its consequences.

Kallen and Noortwijk (2005) presented a risk based inspection technique (RBI) technique that develops cost and safety optimal inspection plan. A periodic inspection and replacement policy, which minimizes the expected average costs per year, is found.

Krishnasamy, Khan and Haddara (2005) developed maintenance strategy based on risk for a power generating plant. Applying this risk based maintenance methodology results in risk reduction , increases the reliability and reduces the cost of maintenance.

Noori and Price (2005) implemented the semi-quantitative risk based inspection approach developed by the American Petroleum Institute (API) on furnace tubes. The calculated 5x5 risk matrix is used in determining the highest risk category for the tubes to take the priority in planning the inspection program.

Straub and Faber (2005) presented a new risk based inspection approach. The presented approach is an integral approach that considers entire systems in inspection planning, while most of the risk based inspection approaches focus exclusively on individual components or have considered system effects in a very simplified manner only.

Khan, Haddara, and Battacharya (2006) developed a risk based methodology for integrity and inspection modeling (RBIIM). The methodology presents quantitative risk based inspection approaches that use the gamma stochastic process to model the corrosion damage mechanism and Bayes's theorem to update knowledge over the corrosion rate. The proposed methodology gives a periodic inspection and replacement policy that minimizes the expected average cost per year.

Review of Selecting an Optimum Inspection Technique / an optimum technique and its associated inspection interval

Chung, et al. (2006) suggested a model for developing an optimal selection of a NDI technique and its associated inspection interval. They formulated a total cost function that includes the cost of inspections over the lifetime and the cost of failure but does not include the cost of repairs. Probability of failure was defined as the probability of failure to detect a growing crack before reaching the critical size. The selection of an optimal NDI technique and its associated inspection interval was based on the minimum total cost and keeping the probability of failure below a predefined limit (safety constraint).

Schueller and Kuntiyawichai (2006) proposed a reliability based optimization approach for NDI planning. The total cost function includes the cost of inspections, the cost of repairs over the lifetime and the cost of failure. Probability of failure was defined as the probability of a crack reaching the critical size. This probability of failure was obtained as a function of the structural design variables (e.g., thickness), the operation period, and the mean and standard deviation of the initial crack size distribution. The NDI technique which has a minimum total cost under the condition that the probability failure does not exceed a predefined limit was designated the optimal technique..

Rouhan and Schoefs (2003) developed a model for selecting an optimum NDI technique. The cost function was formulated for only one inspection and divided into two parts. The first part includes the cost in case of non-detection (cost of failure and cost of inspection) and the other part includes the cost in case of false detection of a crack that does not exist (cost of false repair). Probability of detection (POD) for each inspection technique was

taken as a constant and not as a function of the crack size. Probability of failure was defined as probability of the existence of a crack, having any size, given that the inspection technique does not detect this crack. The optimal technique was obtained by selecting a technique which gives the minimum cost in the two cases of non-detection and false detection.

1.3 Methodology

The optimization problem is considered as a decision making problem. The decision variables are:

i. Type of the NDI technique (e.g. Ultrasonic Inspection, Radiographic Inspection) which can be quantitatively represented by reliability of the inspection technique (Probability of Detection "POD" and Probability of False Calls "PFC").

ii. The inspection interval.

The constraint of the optimization problem is probability of failure to be kept less than a predefined limit (safety constraint).

We aim at obtaining a quantitative methodology for solving this optimization problem or in other words finding the optimum decision variables which minimize the total cost (objective function). The formulated objective function includes cost of inspections, cost of repairs over the lifetime and risk of failure. POD of the inspection technique is taken as a function of the crack size while the crack size is a function of the time as a result of the cyclic loading fatigue. Probability of failure is defined as probability of failure to detect a growing crack before reaching the critical size. The optimal selection of NDI technique

and associated inspection interval was obtained at the minimum value of the objective function keeping probability of failure not exceeding a predefined limit. The proposed model is explained in details in Chapter 5.

1.4 Organization of the Thesis

The thesis consists of seven chapters. Chapter 1 provides a statement of the objectives of the work, a brief review of the literature, and outlines the research methodology which has been followed in the thesis. Chapter 2 describes the different kinds of materials discontinuities and flaws, the purpose and goal of nondestructive inspection methods, issues related to nondestructive inspection, and acceptance criteria. The most common NDI techniques used for detecting these material discontinuities are introduced in Chapter 3. Chapter 4 discusses the estimation of the crack growth rate as a result of loading and environmental conditions. This chapter further illustrates why cracks are considered more harmful than other kind of material discontinuities. The newly developed methodology for optimum nondestructive inspection is explained in Chapter 5. Chapter 6 shows how the analysis is applied in real life. Two relevant and realistic case studies involving welded joints are worked out. Finally, Chapter 7 provides a discussion of the results and conclusions derived from the study.

Chapter 2

Materials Discontinuities

Engineering materials are composed of atoms and molecules that ideally have material continuity extending down into the microscopic scale. Uniformity of material and material properties is desired for most engineering applications. Design engineers assume

some level of structural continuity, homogeneity, and definition of material properties. However, absolute homogeneity and continuity does not usually exist in any engineering component. This chapter describes the different kinds of materials discontinuities and flaws. One of the primary goals of nondestructive inspection is to determine whether or not the discontinuities are acceptable. Accurate estimates of the size, location, and orientation of a discontinuity is most helpful and sometimes critical in the prevention of an impending failure.

Spatially sharp departures from material homogeneity and continuity inside a component at any level of magnification are called discontinuities. Engineering materials always possess some discontinuities, which can be acceptable or not acceptable depending on the application. Examples of these discontinuities include voids, inclusions, laps, cracks, and local changes in microstructural features (e.g. arrangement of atoms and molecules, grain size, shape and orientation) which in turn affect on the behavior of the material in terms of physical properties (e.g., strength, toughness, ductility, hardness, corrosion resistance, wearability).

Discontinuities in engineering components are unacceptable when they degrade the performance or durability of the structure below the expectations of design and when they challenge the operability, reliability, and life of a component. An evaluation of a discontinuity is usually made in reference to a design basis and may include a code or rule-based criteria for acceptance and rejection (for example, ASME Boiler and Pressure Vessel Code, Section XI, 2004 Edition). The evaluation of a discontinuity generally requires an adequate measurement of its size and location and identification of its

character. Discontinuities are evaluated by determining their location, number, shape, size, orientation, and type. Often, in NDI and Quality control anomaly, discontinuity, defect, flaw, cracks, imperfection, non-conformance are the terms used when the material/component tested deviates from requirement/ideality. An imperfection is a condition of being imperfect or a departure of a required condition or specification [Deardorff (2002)]. The term 'flaw' means a detectable unintentional discontinuity or a detectable imperfection in a physical or dimensional attribute of a part. A planar breach in continuity in a material is called a crack. The term 'nonconforming' means only that a part is deficient in one or more specified characteristics. If a flaw (imperfection or unintentional discontinuity) of such type, size, location, shape and/or orientation is unacceptable for continued service or unable to meet minimum applicable acceptance standards or specifications, it is called a defect. The term "defect" designates rejectability. Because in this chapter we are examining these phenomena outside the requirements of any specific code or standard, and we will not be discussing their limitations, we will use the term discontinuities or flaws.

The origin and types of discontinuities depend primarily on the manufacturing processes and the service histories of engineering components. In some cases, the operational environment may induce the growth and development of preexisting discontinuities.

Discontinuities may originate at any manufacturing step and may be introduced during the component use.

An understanding of the origin of discontinuities is useful in determining the type and features of discontinuities that may be expected in a component.

2.1 Classification of Materials Discontinuities

Discontinuities may be classified by the stage in processing at which they are introduced as shown in Fig. 2.1 [Charles, 2003]:

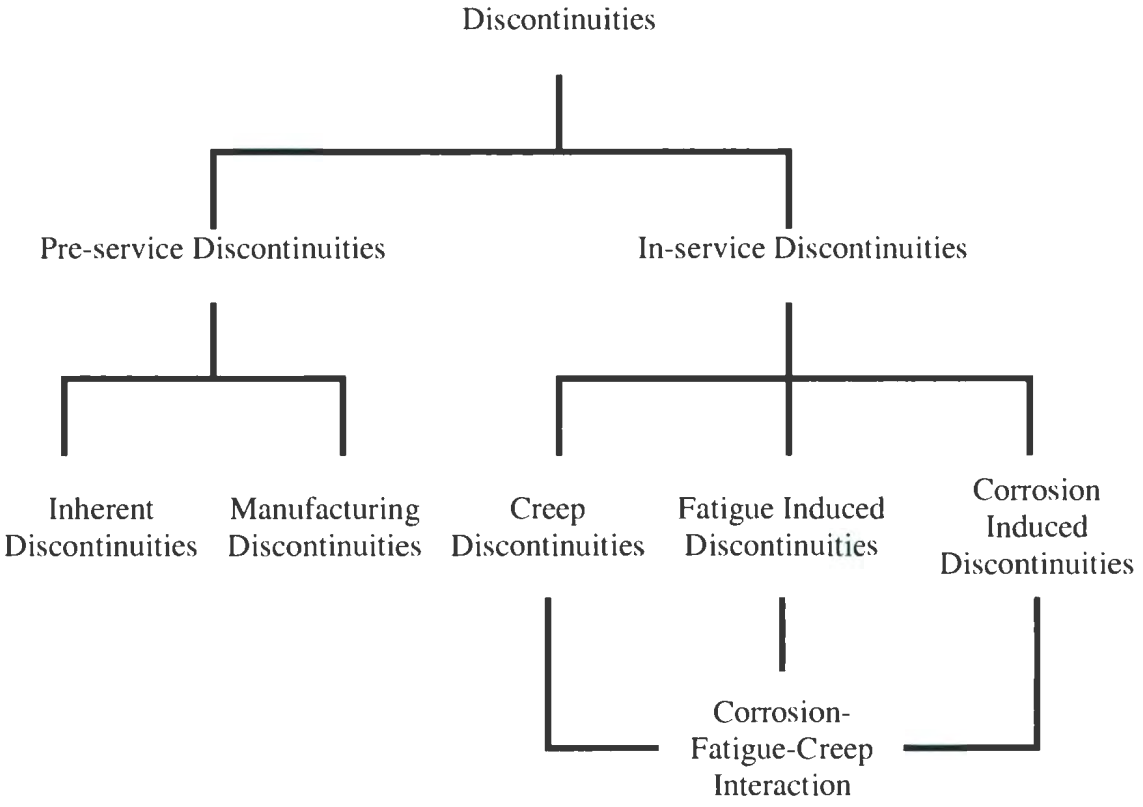

Fig. 2.1: Classification of Materials Discontinuities

2.1.1 Pre-service discontinuities

a) Inherent discontinuities

Discontinuities that are generated in the extraction of raw material. The extraction of metals from ores requires processes that often carry over some of impurities from the rocks and chemical additions used in the refinement process.

b) Manufacturing discontinuities

Discontinuities that are generated in the first forming steps of an alloy or generated in subsequent forming or manufacturing steps (e,g., casting, forging, rolling, extrusion, welding). Casting is usually done in the primary production of metals and in the initial production of alloys. Casting is the starting point for many discontinuities in engineering components. Forms of casting discontinuities include voids, shrinkage porosity, gas porosity, slag and shrinkage cracks. During forging operation, material will lap over itself. The folded material will not fuse if the temperature is low and if the surface is contaminated with dirt. This type of discontinuity is called a fold or a lap. In forging operation, it is possible that the stress resulting from forming load may exceed the strength of the material causing the material to break apart. This load induced cracking is called a burst. Other forming techniques such as rolling and extrusion may generate some discontinuities such as cracks, laps and burst.

During welding process, there are discontinuities within or adjacent to the weld. Common welding discontinuities are:

i. *Incomplete penetration (IP) or lack of penetration (LOP)* occurs when the weld metal fails to penetrate the joint. It is one of the most objectionable weld discontinuities. Lack of penetration allows a natural stress riser from which a crack may propagate. (Fig. 2.2).

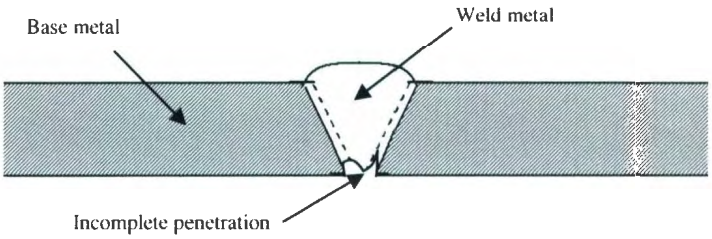

Fig. 2.2: Incomplete penetration in a welding joint

ii. *Incomplete fusion* is a condition where the weld metal does not properly fuse with the base metal (Fig. 2.3).

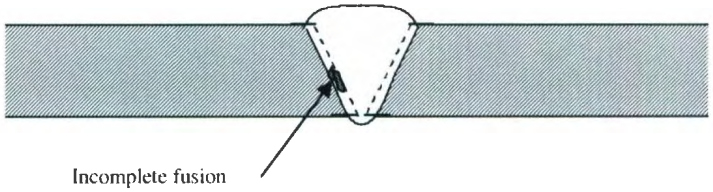

Fig. 2.3: Incomplete fusion in a welding joint

iii. *Slag inclusions* are nonmetallic solid material entrapped in weld metal or between weld and base metal (Fig. 2.4).

Fig. 2.4: Slag inclusions in a welding joint

iv. *Porosity* is the result of gas entrapment in the solidifying metal. This is the result of gas attempting to escape while the metal is still in a liquid state (Fig. 2.5).

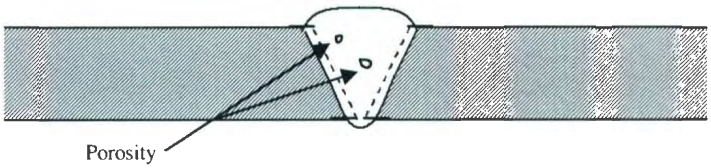

Fig. 2.5: Porosity in a welding joint

v. *Internal concavity or suck back* is a condition where the weld metal has contracted as it cools and has been drawn up into the root of the weld (Fig. 2.6).

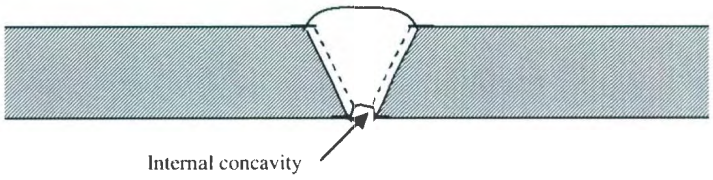

Fig. 2.6: Internal concavity in a welding joint

vi. *Internal or root undercut* is an erosion of the base metal next to the root of the weld. (Fig. 2.7).

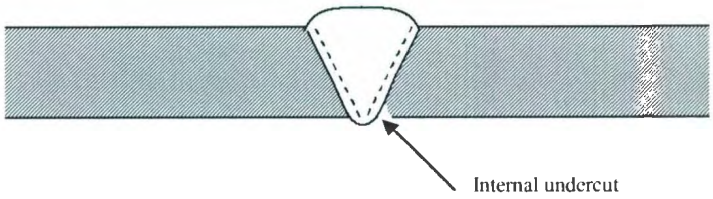

Fig. 2.7: Internal or root undercut in a welding joint

vii. *External or crown undercut* is an erosion of the base metal next to the crown of the weld (Fig. 2.8).

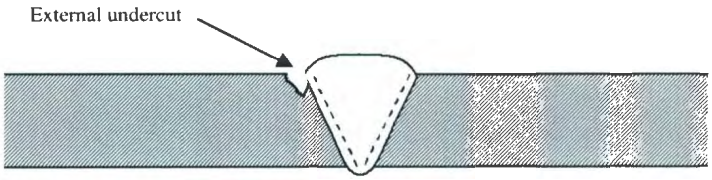

Fig. 2.8: External or crown undercut in a welding joint

viii. *Offset or mismatch* is term associated with a condition where two pieces being welded together are not properly aligned (Fig. 2.9).

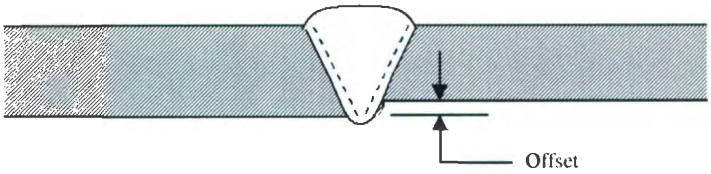

Fig. 2.9: Offset or mismatch in a welding joint

ix. *Inadequate weld reinforcement* is an area of a weld where the thickness of weld metal deposited is less than the thickness of the base material (Fig. 2.10).

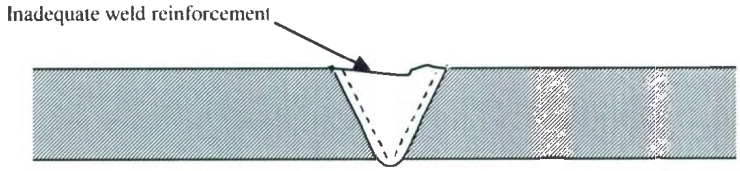

Fig. 2.10: Inadequate weld reinforcement in a welding joint

x. *Excess weld reinforcement* is an area of a weld that has weld metal added in excess of that specified by engineering drawings and codes (Fig. 2.11).

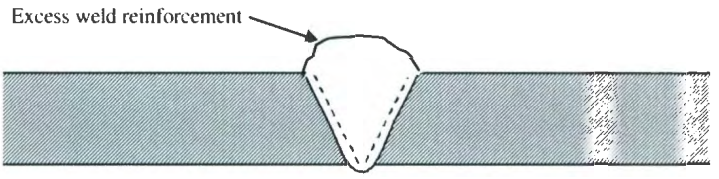

Fig. 2.11: Excess weld reinforcment in a welding joint

xi. *Cracks* are considered more harmful (Fig. 2.12).

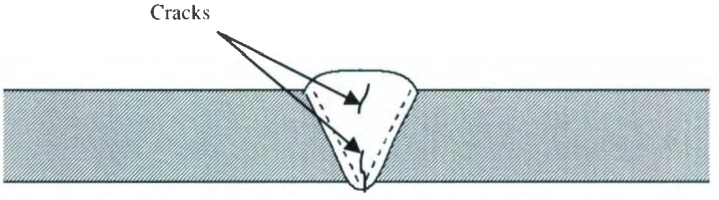

Fig. 2.12: Cracks in the radiograph of welding joint

xii. *Oxide inclusions* are usually visible on the surface of material being welded (Fig. 2.13)

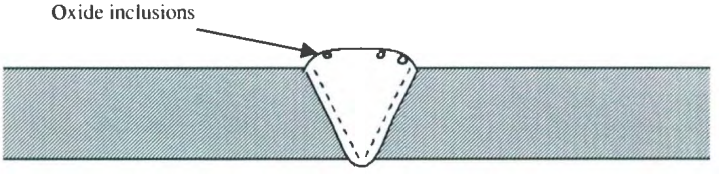

Fig. 2.13: Oxide inclusions in the radiograph of welding joint

xiii. *Cold lap* is a condition where the weld metal does not properly fuse with the base metal or the previous weld pass material (interpass cold lap) causes slightly molten puddle to flow into the base material without bonding (Fig. 2.14).

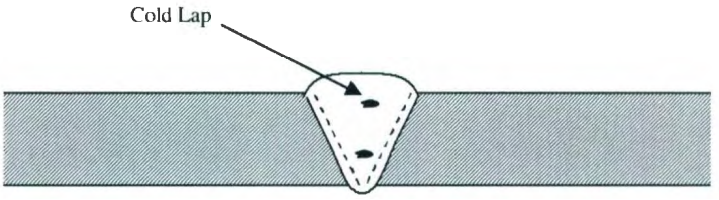

Fig. 2.14: Cold lap in a welding joint

2.1.2 In-Service Discontinuities

2.1.2.1 Fatigue Induced Discontinuities

a) Cyclic Loading Fatigue (Mechanical Fatigue)

Cyclic loading fatigue (mechanical fatigue), also simply known as fatigue is an extremely common failure mode and deserves considerable attention because it can inflict damage on a material at a stress level that is far less than the material's design limit.

A material that fractures after being subjected to a cyclic stress (fluctuating load) over a period of time is considered to have failed by fatigue. The maximum value of the cyclic stress (stress amplitude) for fatigue failure is less than the material's ultimate tensile strength. It is often the case that the maximum value of the cyclic stress is so low that if it were applied at a constant level the material would be able to easily support the load without incurring any damage. Cyclic loads cause the initiation and growth of a crack up to the material fractures when the crack is significant enough such that the material can no longer support the load.

The fatigue failure mechanism involves three stages: crack initiation, crack propagation, and material rupture. Similar to both ductile and brittle fracture, fatigue cracks are often initiated by material discontinuities. These discontinuities or initiation points act as stress raisers where the applied stress concentrates until it exceeds the local strength of the material and produces a crack. The best way to prevent fatigue failure is to keep fatigue cracks from initiating, which can be accomplished by removing or minimizing crack initiators, or by minimizing the stress amplitude. Once fatigue cracks have been initiated they will seek out the easiest or weakest path to propagate through the material. Therefore, minimizing the number of internal material discontinuities, such as voids and inclusions, will increase the time it takes a crack to propagate. Finally, when the crack has weakened the material to a point such that it can no longer support the applied load it will rupture.

Fatigue is not so much dependent on the time as it is on the number of cycles. A cycle consists of an applied stress being increased from a starting value (in some cases, zero or negative) up to a maximum positive value (material loaded in positive direction) and then decreasing past the starting point down to a minimum value (in some cases this is a maximum negative loading), and finally back up to the starting value. This cycle is illustrated in Fig. (2.15) where there is positive and negative loading. Moreover, the stress cycles do not need to be symmetric, but can be randomly changing. Ferrous or iron alloy materials do have a fatigue (endurance) limit, which is the stress level (amplitude) under which no failure will

occur regardless of the number of cycles. On the other hand, by increasing the stress amplitude, the fatigue failure will commence after a smaller number of cycles.

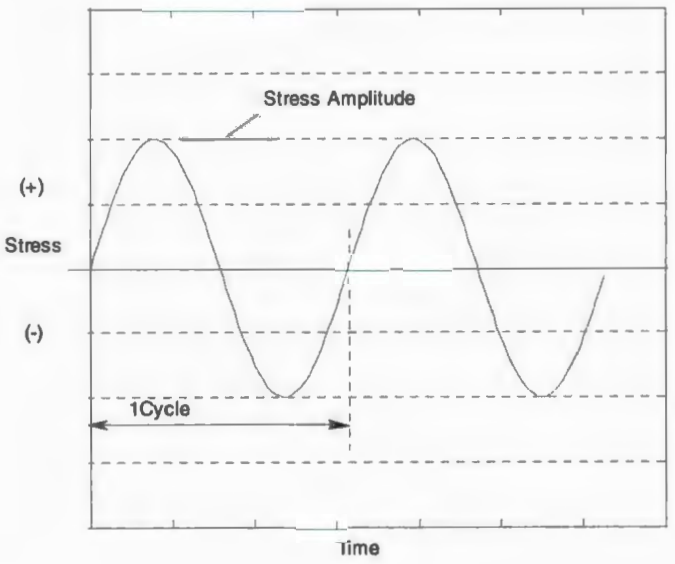

Fig. 2.15: Fatigue Loading Cycles

b) Thermal Fatigue

Simple temperature fluctuations or repeated heating and cooling can impose stresses on a material leading to fatigue damage and potentially failure. Materials generally exhibit a dimensional change or strain to some extent in response to temperature changes. This response can be significant in some materials, especially metals, and can induce thermal stresses on the material if it is mechanically confined in some way. When a material is exposed to conditions of fluctuating temperatures it can cause cyclic fatigue loading, which can result in crack growth and possibly fracture. This process is referred to as thermal fatigue.

Mechanical loading is not required for thermal fatigue to occur, and this failure mode is different from fatigue under fluctuating stress at high temperature. If there is a temperature gradient within the material that is exposed to fluctuating temperatures, it may experience thermal fatigue since different sections of the material's microstructure will respond unequally to the temperature changes. Failure from thermal fatigue can occur not only from fracture but also from a permanent change in shape.

Thermal fatigue is a significant concern in certain applications such as internal combustion engines, heat exchangers, and turbine engine blades.

2.1.2.2 Creep Discontinuities

High temperature operation of metals and alloys for long periods of time may generate an in-service induced cracking called creep cracking. This condition may occur even if the stresses are relatively low. The cracks are usually preceded by discontinuities in the form of creep voids which are small and distributed. The creep voids grow and then cracking links these voids.

2.1.2.3 Corrosion Induced Discontinuities

Corrosion is the deterioration of a metal or alloy and its properties due to a chemical or electrochemical reaction with the surrounding environment. The most serious consequence of corrosion is a component or system failure. Failure can occur either by sufficient material property degradation, such that the component or structure is

rendered unable to perform its intended function, or by fracture that originates from or is propagated by corrosive effects.

While corrosion manifests itself in many different forms and through various environments and mechanisms, only the most significant forms are discussed in this chapter. The following sections contain discussions on failures resulting from uniform, galvanic, crevice, pitting, intergranular, erosion corrosion, hydrogen damage and stress corrosion cracking. In addition to discussions on corrosion-fatigue interaction (corrosion fatigue) and creep-fatigue interaction.

a) Uniform Corrosion (General Corrosion)

Uniform corrosion (general corrosion) is a generalized corrosive attack that occurs over a large surface area of a material. The result is a thinning of the material until failure occurs. Uniform corrosion can also lead to changes in surface properties such as increased surface roughness and friction, which may cause component failure especially in the case of moving parts that require lubricity.

In most cases corrosion is inevitable. Therefore, mitigating its effects or reducing the corrosion rate is essential to ensuring material longevity. Protecting against uniform corrosion can often be accomplished through selection of a material that is best suited for the anticipated environment. The selection of materials for uniform corrosion resistance should simply take into consideration the susceptibility of the metal to the type of environment that will be encountered. Aside from selecting a material that is resistant to uniform

corrosion, protection schemes such as organic or metallic coatings can be implemented wherever feasible. There are also coatings where additional elements, such as chromium, are incorporated for corrosion resistance. When coatings are not used, surface treatments that artificially produce the metal oxide layer prior to exposure to the environment will result in a more uniform layer with a controlled thickness. A uniform oxide layer can provide effective corrosion resistance for some materials.

Also, vapor phase inhibitors may be used in such applications as boilers to adjust the pH level of the environment, thus reducing the rate of corrosion.

b) Galvanic Corrosion

Galvanic corrosion is a form of corrosive attack that occurs when two dissimilar metals (e.g. stainless steel and magnesium) are electrically connected, either through physically touching each other or through an electrically conducting medium, such as an electrolyte. When this occurs, an electrochemical cell can be established, resulting in an increased rate of oxidation of the more anodic material (lower electrical potential). The opposing metal, the cathode, will consequently receive a boost in its resistance to corrosion. Galvanic corrosion is usually observed to be greatest near the surface where the two dissimilar metals are in contact.

There are a number of driving forces that influence the occurrence of galvanic corrosion and the rate at which it occurs.

Among these influencing factors are the difference in the electrical potentials of the coupled metals, the relative area of each metal, the system geometry, and the environment to which the system is exposed.

c) Crevice Corrosion

Crevice corrosion occurs as a result of water or other liquids getting trapped in localized stagnant areas creating an enclosed corrosive environment. This commonly occurs under fasteners, gaskets, washers and in joints or in other components with small gaps. Crevice corrosion can also occur under debris built-up on surfaces, sometimes referred to as "poultice corrosion". Poultice corrosion can be quite severe, due to a gradually increasing acidity in the crevice area.

Several factors including crevice gap width, depth, and the surface ratios of materials affect the severity or rate of crevice corrosion. Tighter gaps, for example, have been known to increase the rate of crevice corrosion of stainless steels in chloride environments. The larger crevice depth and greater surface area of metals will generally increase the rate of corrosion.

To protect against problems with crevice corrosion, systems should be designed to minimize areas likely to trap moisture, other liquids, or debris. For example, welded joints can be used instead of fastened joints to eliminate a possible crevice. Where crevices are unavoidable, metals with a greater resistance to crevice corrosion in the intended environment should be selected. Crevice areas

should be sealed to prevent the ingress of water. Also, a regular cleaning schedule should be implemented to remove any debris build up.

d) Pitting Corrosion

Pitting corrosion, also simply known as pitting, is an extremely localized form of corrosion that occurs when a corrosive medium attacks a metal at specific points causing small holes or pits to form.

This usually happens when a protective coating or oxide film is perforated, due to mechanical damage or chemical degradation. Pitting can be one of the most dangerous forms of corrosion because it is difficult to anticipate and prevent, relatively difficult to detect, occurs very rapidly, and penetrates a metal without causing it to lose a significant amount of weight. Failure of a metal due to the effects of pitting corrosion can occur very suddenly. Pitting can have side effects too, for example, cracks may initiate at the edge of a pit due to an increase in the local stress.

e) Intergranular Corrosion

Intergranular corrosion attacks the interior of metals along grain boundaries. It is associated with impurities, which tend to deposit at grain boundaries, and/or a difference in crystallographic phase precipitated at grain boundaries. Heating of some metals can cause a "sensitization" or an increase in the level of inhomogeniety at grain boundaries. Therefore, some heat treatments and weldments can result in a propensity for intergranular corrosion. Some metals

may also become sensitized while in operation if used at a high enough temperature to cause such changes in internal crystallographic structure.

Intergranular corrosion can occur in many alloys, but stainless steels, as well as some aluminum and nickel-based alloys, are predominantly susceptible. Stainless steels, especially ferritic stainless steels, have been found to become sensitized, particularly after welding. Aluminum alloys also suffer intergranular attack as a result of precipitates at grain boundaries that are more active.

f) Erosion Corrosion

Erosion corrosion is a form of attack resulting from the interaction of an electrolytic solution in motion relative to a metal surface. It has typically been associated with small solid particles dispersed within a liquid stream. The fluid motion causes wear and abrasion, increasing rates of corrosion over uniform (non-motion) corrosion under the same conditions.

Erosion corrosion is evident in pipelines, cooling systems, valves, boiler systems, propellers, impellers, as well as numerous other components. Specialized types of erosion corrosion occur as a result of impingement and cavitation. Impingement refers to a directional change of the solution, whereby a greater force is exhibited on a surface such as the outside curve of an elbow joint. Cavitation is the phenomenon of collapsing vapor bubbles, which can cause surface damage if they repeatedly hit one particular location on a metal.

There are several factors that influence the resistance of a material to erosion corrosion including hardness, surface smoothness, fluid velocity, fluid density, angle of impact, and the general corrosion resistance of the material to the environment.

Materials with higher hardness values typically resist erosion corrosion better than those that have a lower value.

g) Hydrogen Damage

There are a number of different ways that hydrogen can damage metallic materials, resulting from the combined factors of hydrogen and residual or tensile stresses. Hydrogen damage can result in cracking, embrittlement, loss of ductility, blistering and flaking, and microperforation.

Hydrogen induced cracking (HIC) refers to the cracking of a ductile alloy when under constant stress and where hydrogen gas is present. Hydrogen is absorbed into areas of high stress producing the observed damage. A related phenomenon, hydrogen embrittlement, is the brittle fracture of a ductile alloy during plastic deformation in a hydrogen gas containing environment.

In both cases, a loss of tensile ductility occurs with metals exposed to hydrogen which results in a significant decrease in elongation and reduction in area. It is most often observed in low strength alloys, but also occurs in steels, stainless steels, aluminum alloys, nickel alloys, and titanium alloys.

Another form of damage occurs when high pressure hydrogen attacks carbon and low-alloy steels at high temperatures. The hydrogen will diffuse into the metal and react with carbon resulting in the formation of methane. This in turn results in decarburization of the alloy and possible crack formation.

h) Stress Corrosion Cracking

Stress corrosion cracking (SCC) is an environmentally induced cracking phenomenon that sometimes occurs when susceptible metals are subjected to a tensile stress and a corrosive environment simultaneously. This is not to be confused with similar phenomena such as hydrogen embrittlement, in which the metal is embrittled by hydrogen, often resulting in the formation of cracks. Moreover, SCC is not defined as the cause of cracking that occurs when the surface of the metal is corroded resulting in the creation of a nucleating point for a crack. Rather, it is a synergistic effort of a corrosive agent and a static stress. Another form of corrosion similar to SCC, although with a subtle difference, is corrosion fatigue. The key difference is that SCC occurs with a static stress, while corrosion fatigue occurs under a dynamic or cyclic stress.

Stress corrosion cracking is a process that takes place within the material, where the cracks propagate through the internal structure, usually leaving the surface unharmed [Fang, et. al. (2002)]. Aside from an applied mechanical stress, a residual, thermal, or welding stress along with the appropriate corrosive agent may also be sufficient to promote SCC. Stress corrosion cracking is a dangerous

form of corrosion because it can be difficult to detect, and it can occur at stress levels which fall within the range that the metal is designed to handle.

Stress corrosion cracking is dependent on environmental factors including temperature, solution, and stress, as well as the metallic structure and composition. However, certain types of alloys are more susceptible to SCC in particular environments, while other alloys are more resistant to that same environment. Increasing the temperature of a system often works to accelerate the rate of SCC. The presence of chlorides or oxygen in the environment can also significantly influence the occurrence and rate of SCC [Gooch, T. G. (1986)].

The magnitude of SCC can be measured experimentally based on a rate of crack propagation. This measure identifies how quickly a material may fail under an applied load in corrosive conditions. The susceptibility of a material to SCC may also be estimated based on a critical stress value that will propagate a crack under corrosive conditions. This factor is called the stress corrosion cracking stress intensity factor, K_{ISCC} which quantifies the phenomenon as it is the case in fatigue crack growth (FCG) which can be quantified using the stress intensity factor for fatigue crack growth, K_{IFCG}, (for fatigue crack growth assessment, see Chapter 4). K_{ISCC} is dependent on material properties and it can be directionally dependent, and the designer or engineer needs to be careful in applying it to the proper direction of the material under consideration. Furthermore, K_{ISCC} is

environmentally dependent, and as a result the environment in which the test data was produced should be taken into consideration.

2.1.2.4 Corrosion-Fatigue-Creep Interaction

In some applications, there is an interaction between two or more degradation mechanisms (fatigue, corrosion and creep). For example, corrosion fatigue and creep-fatigue interaction as explained below:

a) Creep-Fatigue Interaction

At elevated temperatures creep and fatigue can act simultaneously to produce a concerted, harmful effect on a material. A material operating in high temperature conditions can experience both creep strains and cyclic strains that can seriously affect the material's lifetime. For example, if a material experiences creep strains while undergoing fatigue cycling, its fatigue life can be greatly reduced. Similarly, if a material experiences fatigue cycling while undergoing creep, its creep life can be significantly reduced.

b) Corrosion Fatigue

Corrosion fatigue is the environmentally-assisted mechanical degradation of a material due to the combined effects of corrosion and fatigue (a direct result of cyclic stress loading).

SCC occurs under static stress while corrosion fatigue occurs under a cyclic stress (part of which is tensile stress). Corrosion fatigue is a potential cause for the failure of many types of metals and alloys in various types of environments.

Materials that experience corrosion fatigue essentially exhibit a decrease in fatigue strength due to the effects of electrochemical degradation (corrosive environment). The stress required for both crack initiation and propagation is lower in corrosive environments.

The crack growth rate can be much higher in a corrosive environment than it is in a non-corrosive environment. Therefore, the fatigue life of a material is shortened if it is simultaneously exposed to a corrosive environment and fatigue conditions.

Chapter 3

Non-Destructive Inspection (NDI) Techniques

This chapter provides a review of the most common non-destructive inspection techniques such as ultrasonic, magnetic, radiographic and thermal inspection. Effectiveness, advantages, disadvantages, main uses, and limitations of these techniques are also discussed in this chapter. This information is subsequently used in the proposed optimization model (Chapter 5) for selecting an optimum NDI technique and its associated optimum inspection interval. The general definition of nondestructive inspection (NDI) is an examination that is performed on an object to determine the absence or presence of flaws that may have an effect on the usefulness or serviceability of that object or to measure other object characteristics (e.g. size, dimension, alloy content) [Charles 2003]. Nondestructive examination (NDE), nondestructive evaluation (NDE) and nondestructive testing (NDT) are also expressions commonly used to describe this technology [Charles 2003]. Although NDI cannot guarantee that failures will not occur, it plays a significant role in minimizing the possibilities of failure.

A variety of NDI techniques are available for detection and characterization of defects in materials. All NDI techniques are based on physical principles. Nearly every form of energy is used as probing medium in NDI. Likewise nearly every property of the materials to be inspected has been made the basis for some method or technique of NDI. In general, NDI methods involve subjecting the material (being examined) to some form of external energy source (e.g. X-rays, ultrasonic, thermal wave, electromagnetic fields) and analyzing the detected response signals (refracted energy, induced voltage and diffracted energy).

NDI techniques can be used for: [Charles 2003]

i. Flaw detection and evaluation

ii. Leakage detection

iii. Location determination

iv. Dimensional measurements

v. Structure and microstructure characterization

vi. Estimation of mechanical and physical properties

vii. Strain and dynamic response measurements

viii. Material sorting and chemical composition determination

3.1 Nondestructive Versus Destructive Tests

Destructive testing has been defined as a form of mechanical test (primarily destructive) of materials where by certain specific characteristics of the material can evaluated

quantitatively. In some cases, the test specimens being tested are subjected to controlled conditions that simulate service. Such destructive tests can provide very useful information, especially relating to the material's design considerations and useful life. Destructive testing may be dynamic or static. It provides data relative to the material attributes such as ultimate tensile strength, yield point, ductility, elongation characteristics, fatigue life, corrosion resistance, toughness, and impact resistance.

Although it is assumed in many cases that the test specimen is representative of the material from which it has been taken, it cannot be said with 100% reliability that the balance of the material will have exactly the same characteristics as that test specimen. Key benefits of destructive testing include:

i. Reliable and accurate data from the test specimen

ii. Extremely useful data for design purposes

iii. Information can be used to establish standards and specifications

iv. Data achieved through destructive testing is usually quantitative

v. Typically, various service conditions are capable of being measured

vi. Useful life can generally be predicted

Limitations of destructive testing include:

i. Data applies only to the specimen being examined

ii. Most destructive test specimen cannot be used once the test is complete

iii. Many destructive test require large, expensive equipment in a laboratory environment

Benefits of nondestructive testing include:

i. The part is not changed or altered and can be used after examination

ii. Every item or a large portion of the material can be examined with no adverse consequences

iii. Material can be examined for conditions internal and at the service

iv. Parts can be examined while in service

v. Many NDI methods are portable and can be taken to the object to be examined

vi. Nondestructive testing is cost effective

Limitations of nondestructive testing include:

i. It is usually quite operator dependent

ii. NDI methods do not generally provide quantitative data

iii. Orientation of flaws must be considered

iv. Evaluation of some test results are subjective and subject to dispute

v. While most methods are cost effective, some, such as radiography, can be expensive

vi. Defined procedures that have been qualified are essential

vii. It is usually quite dependent on operator qualification.

In conclusion, there are obvious benefits for requiring both nondestructive and destructive testing. Each is capable of providing extremely useful information, and when used jointly can be very valuable to the designer when considering useful life and application of the part.

3.2 Most Common NDI Techniques [Charles (2003)]

3.2.1 Visual Inspection

Visual inspection plays an important role in quick assessment of the quality of the inspected component and to identify various defects. Developments in image processing, artificial intelligence, video technology and other related fields have significantly improved the capability of visual techniques. Present day demand for higher performance and faster production exceed the abilities of visual tests by humans. Consequently, visual inspections made by human eye are being replaced by automated visual inspection using optical instruments and unstaffed inspection stations. Such aspects are usually referred to as machine vision.

3.2.1.1 Instruments for Visual Inspection

The human eye is an excellent sensor and with that, it is possible to easily perceive many material characteristics (eg. shapes, colours, gloss, shades) and examining cleanliness, misalignments and other mismatches, foreign objects. The human eye is an important component for performing visual NDI.

Optical aids (eg. Borescopes, fiberscopes, videoimagescopes) are usually recommended for visual inspection, essentially for magnification purpose and also for inspecting the

inaccessible areas (e.g inside surfaces of tubes, geometrical imperfections such as weld convexity and concavity of weld joints need to be detected in inaccessible regions). Using the 3-D graphic measurement system, it is possible to measure dimensions such as length and width on the images very accurately

In recent times, with the availability of flexible fibre-optic borescopes, cameras, and computer based image processing software, it is possible to examine corners, bent surfaces, and inaccessible surfaces. Using these instruments, it is possible to take sharp and clear images of parts and interior surfaces and make quantitative evaluations. The diameter and length of the flexiscopes are usually adapted depending on the requirements and the dimensions of the test object. Selection of a visual instrument mainly depends on factors such as the object geometry and the access, expected defect size and resolution requirements.

The five basic elements in a visual test are the test object, the inspector, the optical instrument, illumination and recording. Each of these elements interacts with the others and affects the test results. The objective distance, object size, discontinuity size, reflectivity, entry port size, object thickness and direction of view are all critical aspects of the test object that affect the visual test.

In many situations, in order to aid vision, magnification with power ranging from 1.5X to 2000X is employed. Depending on the working distance and the field of view various lower, medium and high power magnification systems (microscopes) are used. With high power systems, it would be possible to achieve resolution of a few microns. The defect size usually determines the magnification and resolution required for visual inspection.

For example, greater resolution is required to detect hairline cracks in welds than to detect an undercut.

3.2.2 Penetrant Inspection

Penetrant inspection (liquid penetrant inspection) is a method that is used to reveal surface breaking flaws by bleed out of a colored or fluorescent dye from the flaw. The technique is based on the ability of a liquid to be drawn into a "clean" surface breaking flaw by capillary action. After a period of time called the "dwell," excess surface penetrant is removed and a developer applied. This acts as a blotter. It draws the penetrant from the flaw to reveal its presence. Colored (contrast) penetrants require good white light, while fluorescent penetrants need to be used in darkened conditions with an ultraviolet "black light".

3.2.2.1 Basic Processing Steps of a Penetrant Inspection

i. Surface Preparation: One of the most critical steps of a liquid penetrant inspection is the surface preparation. The surface must be free of oil, grease, water, or other contaminants that may prevent penetrant from entering flaws.

ii. Penetrant Application: Once the surface has been thoroughly cleaned and dried, the penetrant material is applied by spraying, brushing, or immersing the part in a penetrant bath.

iii. Penetrant Dwell: The penetrant is left on the surface for a sufficient time to allow as much penetrant as possible to be drawn from or to seep into a flaw. Penetrant dwell time is the total time that the penetrant is in contact with the part surface.

Dwell times are usually recommended by the penetrant producers or required by the specification being followed. The times vary depending on the application, penetrant materials used, the material, the form of the material being inspected, and the type of flaw being inspected for. Minimum dwell times typically range from five to 60 minutes. Generally, there is no harm in using a longer penetrant dwell time as long as the penetrant is not allowed to dry. The ideal dwell time is often determined by experimentation and may be very specific to a particular application.

iv. Excess Penetrant Removal: This is the most delicate part of the inspection procedure because the excess penetrant must be removed from the surface of the sample while removing as little penetrant as possible from flaws. This step may involve cleaning with a solvent, direct rinsing with water, or first treating the part with an emulsifier and then rinsing with water.

v. Developer Application: A thin layer of developer is then applied to the sample to draw penetrant trapped in flaws back to the surface where it will be visible. Developers come in a variety of forms that may be applied by dusting (dry powdered), dipping, or spraying (wet developers).

vi. Indication Development: The developer is allowed to stand on the part surface for a period of time sufficient to permit the extraction of the trapped penetrant out of any surface flaws. This development time is usually a minimum of 10 minutes. Significantly longer times may be necessary for tight cracks.

vii. Inspection: Inspection is then performed under appropriate lighting to detect indications from any flaws which may be present.

viii. Clean Surface: The final step in the process is to thoroughly clean the part surface to remove the developer from the acceptable parts.

3.2.2.2 Common Uses of Penetrant Inspection

Penetrant inspection (PI) is one of the most widely used nondestructive inspection (NDI) techniques. Its popularity can be attributed to two main factors: its relative ease of use and its flexibility. PI can be used to detect surface flaws of almost any material provided that its surface is not extremely rough or porous. Materials that are commonly inspected using PI are, for example, metals, glass, many ceramic materials, rubber, plastics.

PI offers flexibility in performing inspections because it can be applied in a large variety of applications. Penetrant materials can be applied with a spray can or a cotton swab to inspect for flaws known to occur in a specific area or it can be applied by dipping or spraying to quickly inspect large areas. One of the major limitations of a penetrant inspection is that flaws must be open to the surface.

3.2.2.3 Advantages and Disadvantages of Penetrant Inspection

Like all nondestructive inspection methods, liquid penetrant inspection has both advantages and disadvantages. The primary advantages when compared to other NDI methods are summarized below [Charles (2003)].

i. The method has high sensitivity to small surface discontinuities.

ii. The method has few material limitations, i.e. metallic and nonmetallic, magnetic and nonmagnetic, and conductive and nonconductive materials may be inspected.

iii. Large areas and large volumes of parts/materials can be inspected rapidly and at low cost.

iv. Parts with complex geometric shapes are routinely inspected.

v. Indications are produced directly on the surface of the part and constitute a visual representation of the flaw.

vi. Aerosol spray cans make penetrant materials very portable.

vii. Penetrant materials and associated equipment are relatively inexpensive.

The primary disadvantages are summarized below:

i. Only surface breaking flaws can be detected.

ii. Only materials with a relatively nonporous surface can be inspected.

iii. Precleaning is critical since contaminants can mask surface flaws.

iv. Metal smearing from machining, grinding, and grit or sand blasting must be removed prior to LPI.

v. The inspector must have direct access to the surface being inspected.

vi. Surface finish and roughness can affect inspection sensitivity.

vii. Multiple process operations must be performed and controlled.

viii. Post cleaning of acceptable parts or materials is required.

ix. Chemical handling and proper disposal is required.

3.2.2.4 Penetrant Inspection Materials

Today's penetrants are carefully formulated to produce the level of sensitivity desired by the inspector. To perform well, a penetrant must possess a number of important characteristics. A penetrant must:

i. Spread easily over the surface of the material being inspected to provide complete coverage.

ii. Be drawn into surface breaking flaws by capillary action.

iii. Remain in the flaw but remove easily from the surface of the part.

iv. Remain fluid so it can be drawn back to the surface of the part through the drying and developing steps.

v. Be highly visible or fluoresce brightly to produce easy to see indications.

vi. Not be harmful to the material being tested or the inspector.

Penetrant materials come in two basic types. These types are listed below:

Type 1 - Fluorescent Penetrants (Fluorescence is the property of a substance, such as fluorite, of producing light while it is being acted upon by radiant energy, such as ultraviolet rays or X-rays)

Type 2 - Visible Penetrants

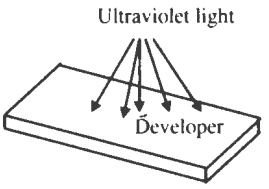

Fig. 3.1: Fluorescent penetrant inspection

Fluorescent penetrants (Fig. 3.1) contain a dye or several dyes that fluoresce when exposed to ultraviolet light (sometimes referred to as "black light"). Visible penetrants (Fig. 3.2) contain a red dye that provides high contrast against the white developer background. Fluorescent penetrant systems are more sensitive than visible penetrant systems because the eye is drawn to the glow of the fluorescing indication. However, visible penetrants do not require a darkened area and an ultraviolet light in order to make an inspection. Visible penetrants are also less vulnerable to contamination from things such as cleaning fluid that can significantly reduce the strength of a fluorescent indication.

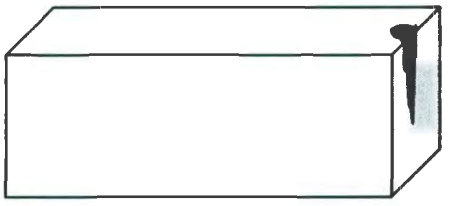

Fig. 3.2: Visible penetrant inspection

3.2.2.5 Developers

The role of the developer is to pull the trapped penetrant material out of flaws and spread it out on the surface of the part so it can be seen by an inspector (Fig. 3.3). The fine developer particles both reflect and refract the incident ultraviolet light, allowing more of

it to interact with the penetrant, causing more efficient fluorescence. The developer also allows more light to be emitted through the same mechanism. Another function that some developers perform is to create a white background so there is a greater degree of contrast between the indication and the surrounding background.

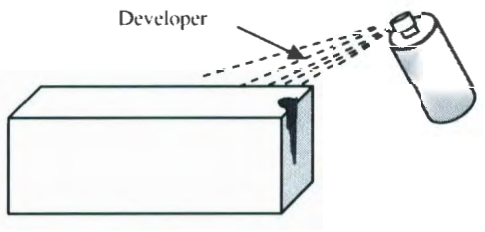

Fig. 3.3: Developer used in penetrant inspection

3.2.2.6 Application of the Penetrant

The application of the penetrant is the step of the process that requires the least amount of control. As long as the surface being inspected receives a generous coating of penetrant, it really doesn't matter how the penetrant is applied. Generally, the application method is an economic or convenience decision.

It is important that the part be thoroughly cleaned and dried. Any contaminates or moisture on the surface of the part or within a flaw can prevent the penetrant material from entering the flaw. The temperature of the inspected surface can have an effect on the result. The recommended range of temperature depends on the properties of the used penetrant.

3.2.3 Magnetic Particle Inspection (MPI) Technique

Magnetic particle inspection (MPI) is a nondestructive inspection technique used for flaw detection. MPI is fast and relatively easy to apply, and part surface preparation is not as

critical as it is for some other NDI techniques. These characteristics make MPI one of the most widely utilized nondestructive inspection methods.

MPI uses magnetic fields and small magnetic particles (i.e. iron filings) to detect flaws in components. The only requirement from an inspectability standpoint is that the component being inspected must be made of a ferromagnetic material such as iron, nickel, cobalt, or some of their alloys. Ferromagnetic materials are materials that can be magnetized to a level that will allow the inspection to be effective.

The method is used to inspect a variety of product forms including castings, forgings, and weldments. Many different industries use magnetic particle inspection for determining a component's fitness-for-use. Some examples of industries that use magnetic particle inspection are the structural steel, automotive, petrochemical, power generation, and aerospace industries. Underwater inspection is another area where magnetic particle inspection may be used to test items such as offshore structures and underwater pipelines.

3.2.3.1 Basic Principles of MPI

In theory, magnetic particle inspection (MPI) is a relatively simple concept. It can be considered as a combination of two nondestructive inspection methods: magnetic flux leakage inspection and visual inspection.

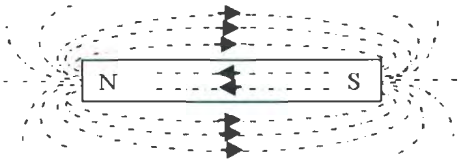

Fig. 3.4: Magnetic field in and around a bar magnet

Consider the case of a bar magnet (Fig. 3.4). It has a magnetic field in and around the magnet. Any place that a magnetic line of force exits or enters the magnet is called a pole. A pole where a magnetic line of force exits the magnet is called a north pole and a pole where a line of force enters the magnet is called a south pole.

When a bar magnet is broken in the center of its length, two complete bar magnets with magnetic poles on each end of each piece will result. If the magnet is just cracked but not broken completely in two, a north and south pole will form at each edge of the crack. The magnetic field exits the north pole and reenters at the south pole (Fig. 3.5).

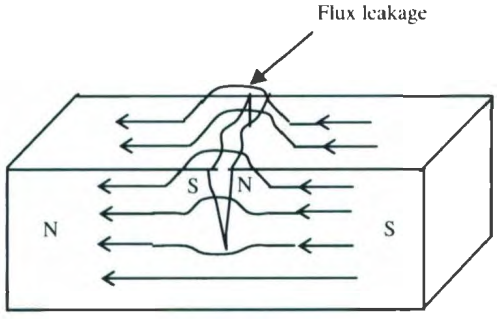

Fig. 3.5: Flux leakage at the crack in magnetic inspection

The magnetic field spreads out when it encounters the small air gap created by the crack because the air cannot support as much magnetic field per unit volume as the magnet can. When the field spreads out, it appears to leak out of the material and, thus is called a flux leakage field.

If iron particles are sprinkled on a cracked magnet, the particles will be attracted to and cluster not only at the poles at the ends of the magnet, but also at the poles at the edges of the crack (Fig. 3.6). This cluster of particles is much easier to see than the actual crack and this is the basis for magnetic particle inspection.

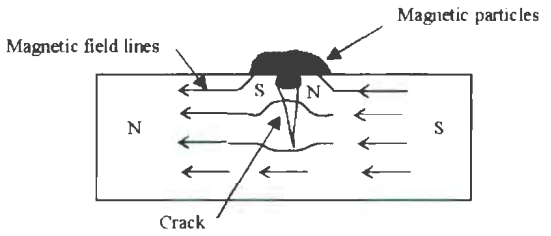

Fig. 3.6: Cluster of iron particles at the edges of the crack in magnetic particle inspection

The first step in a magnetic particle inspection is to magnetize the component that is to be inspected. If any flaws on or near the surface are present, the flaws will create a leakage field. After the component has been magnetized, iron particles, either in a dry or wet suspended form, are applied to the surface of the magnetized part. The particles will be attracted and cluster at the flux leakage fields, thus forming a visible indication that the inspector can detect.

3.2.3.2 Magnetic Field Orientation and Flaw Detectability

To properly inspect a component for cracks or other flaws, it is important to understand that the orientation between the magnetic lines of force and the flaw is very important. There are two general types of magnetic fields that can be established within a component. A longitudinal magnetic field has magnetic lines of force that run parallel to the long axis of the part. Longitudinal magnetization of a component can be accomplished using the longitudinal field set up by a coil or solenoid. It can also be accomplished using permanent magnets or electromagnets (Fig. 3.7).

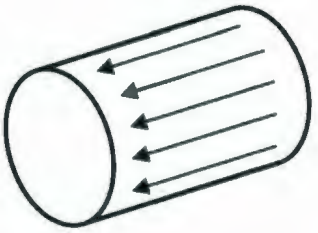

Fig. 3.7: longitudinal magnetic field

A circular magnetic field has magnetic lines of force that run circumferentially around the perimeter of a part. A circular magnetic field is induced in an article by either passing current through the component or by passing current through a conductor surrounded by the component (Fig. 3.8).

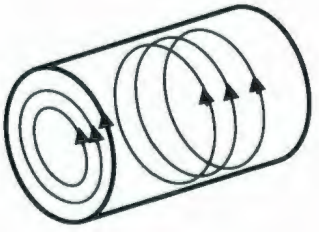

Fig. 3.8: Circular magnetic field

The type of magnetic field established is determined by the method used to magnetize the specimen. Being able to magnetize the part in two directions is important because the best detection of flaws occurs when the lines of magnetic force are established at right angles to the longest dimension of the flaw. This orientation creates the largest disruption of the magnetic field within the part and the greatest flux leakage at the surface of the part. As can be seen in Fig. 3.9, if the magnetic field is parallel to the flaw, the field will see little disruption and no flux leakage field will be produced.

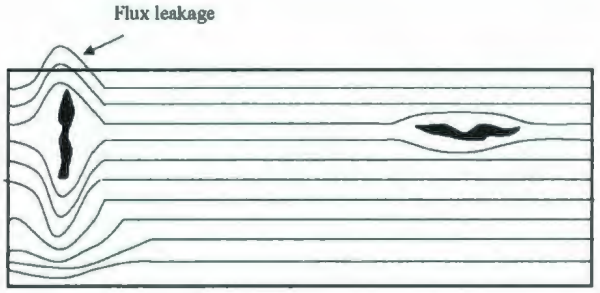

Fig. 3.9: Effect of flaw orientation on detectability using magnetic inspection (longitudinal magnetic field)

An orientation of 45 to 90 degrees between the magnetic field and the flaw is necessary to form an indication. Since flaws may occur in various and unknown directions, each part is normally magnetized in two directions at right angles to each other. If the component below is considered, it is known that passing current through the part from end to end will establish a circular magnetic field that will be 90 degrees to the direction of the current. Therefore, flaws that have a significant dimension in the direction of the current (longitudinal flaws) should be detectable. Alternately, transverse-type flaws will not be detectable with circular magnetization (Fig. 3.10).

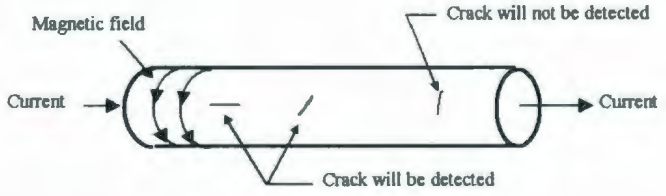

Fig. 3.10: Effect of flaw orientation on detectability using magnetic inspection (circular magnetic field)

3.2.3.3 Magnetization of Ferromagnetic Materials

To properly inspect a part for cracks or other flaws, it is important to become familiar with the different types of magnetic fields and the equipment used to generate them. As discussed previously, one of the primary requirements for detecting a flaw in a ferromagnetic material is that the magnetic field induced in the part must intercept the flaw at a 45 to 90 degree angle. Flaws that are normal (90 degrees) to the magnetic field will produce the strongest indications because they disrupt more of the magnet flux.

Therefore, for proper inspection of a component, it is important to be able to establish a magnetic field in at least two directions. A variety of equipment exists to establish the magnetic field for MPI. Some equipment is designed to be portable so that inspections can be made in the field and some is designed to be stationary for ease of inspection in the laboratory or manufacturing facility.

There are a variety of methods that can be used to establish a magnetic field in a component for evaluation using magnetic particle inspection. It is common to classify the magnetizing methods as either direct or indirect.

3.2.3.4 Magnetization Using Direct Induction (Direct Magnetization)

With direct magnetization, current is passed directly through the component. Recall that whenever current flows, a magnetic field is produced. Using the right-hand rule, it is known that the magnetic lines of flux form normal to the direction of the current and form a circular field in and around the conductor. When using the direct magnetization method, care must be taken to ensure that good electrical contact is established and maintained

between the test equipment and the test component. Improper contact can result in arcing that may damage the component. It is also possible to overheat components in areas of high resistance such as the contact points and in areas of small cross-sectional area.

There are several ways that direct magnetization is commonly accomplished. One way involves clamping the component between two electrical contacts in a special piece of equipment. Current is passed through the component and a circular magnetic field is established in and around the component, Fig. 3.11. When the magnetizing current is stopped, a residual magnetic field will remain within the component. The strength of the induced magnetic field is proportional to the amount of current passed through the component.

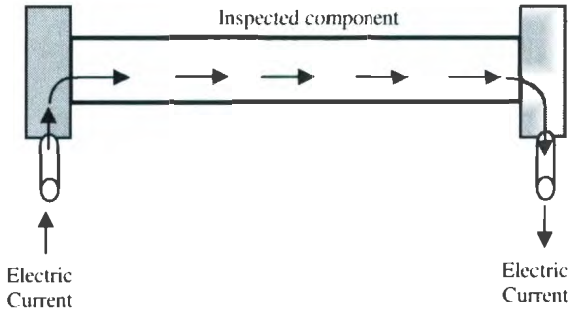

Fig. 3.11: Direct magnetization by clamping the component between two electrical contacts.

A second technique involves using clamps or prods, which are attached or placed in contact with the component, Fig. 3.12. Electrical current flows through the component from contact to contact. The current sets up a circular magnetic field around the path of the current.

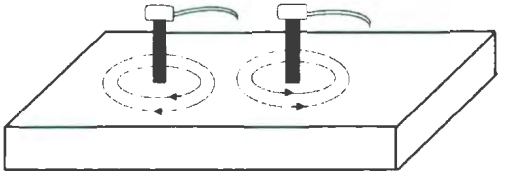

Fig. 3.12: Direct magnetization by placing electrical prods in contact with the component.

3.2.3.5 Magnetization Using Indirect Induction (Indirect Magnetization)

Indirect magnetization is accomplished by using a strong external magnetic field to establish a magnetic field within the component. As with direct magnetization, there are several ways that indirect magnetization can be accomplished.

The use of permanent magnets is a low cost method of establishing a magnetic field. However, their use is limited due to lack of control of the field strength and the difficulty of placing and removing strong permanent magnets from the component.

Electromagnets in the form of an adjustable horseshoe magnet (called a yoke), Fig. 3.13, eliminate the problems associated with permanent magnets and are used extensively in industry. Electromagnets only exhibit a magnetic flux when electric current is flowing around the soft iron core. When the magnet is placed on the component, a magnetic field is established between the north and south poles of the magnet.

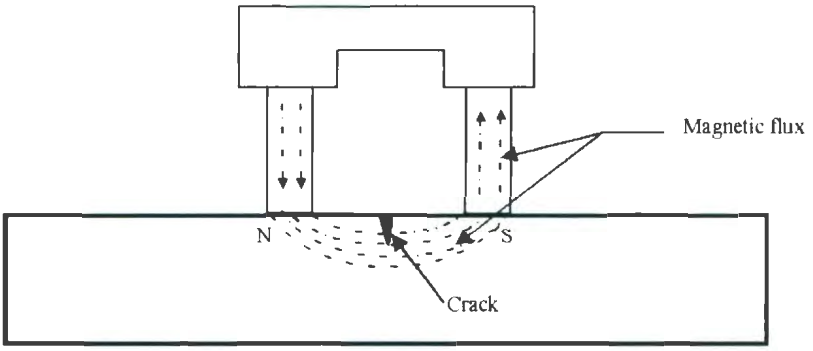

Fig. 3.13: Horseshoe (yoke) electromagnets used for indirect magnetization

Another way of indirectly inducting a magnetic field in a material is by using the magnetic field of a current carrying conductor. A circular magnetic field can be established in cylindrical components by using a central conductor. Typically, one or more cylindrical components are hung from a solid copper bar running through the inside diameter. Current is passed through the copper bar and the resulting circular magnetic field establishes a magnetic field within the test components.

The use of coils and solenoids is a third method of indirect magnetization, Fig. 3.14. When the length of a component is several times larger than its diameter, a longitudinal magnetic field can be established in the component. The component is placed longitudinally in the concentrated magnetic field that fills the center of a coil or solenoid. This magnetization technique is often referred to as a "coil shot."

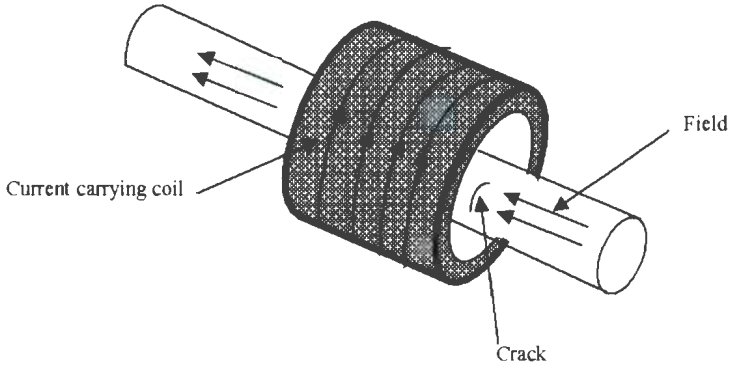

Fig. 3.14: Coils and solenoids used for indirect magnetization

3.2.4 Ultrasonic Inspection Technique

3.2.4.1 Principles of Ultrasonic Inspection

Ultrasonic Inspection (UI) uses high frequency sound energy to conduct examinations and make measurements. Ultrasonic inspection can be used for flaw detection/evaluation, dimensional measurements, material characterization, and more. A typical ultrasonic inspection system is a pulse/echo inspection. This system consists of several functional units, such as the pulser/receiver, transducer, and display devices. A pulser/receiver is an electronic device that can produce high voltage electrical pulses. Driven by the pulser, the transducer generates high frequency ultrasonic energy. The sound energy is introduced and propagates through the materials in the form of waves. When there is a discontinuity (such as a crack) in the wave path, part of the energy will be reflected back from the flaw surface. The reflected wave signal is transformed into an electrical signal by the transducer and is displayed on a screen (Fig. 3.15). The reflected signal strength is displayed versus the time from signal generation to when an echo was received. Signal

travel time can be directly related to the distance that the signal traveled. From the signal, information about the reflector location, size, orientation and other features can be gained.

Another ultrasonic inspection system is to measure changes in ultrasonic wave propagation speed, along with energy losses, from interactions with a material microstructure are often used to nondestructively gain information about a material's properties. Measurements of sound velocity and ultrasonic wave attenuation can be related to the elastic properties that can be used to characterize the texture of polycrystalline metals.

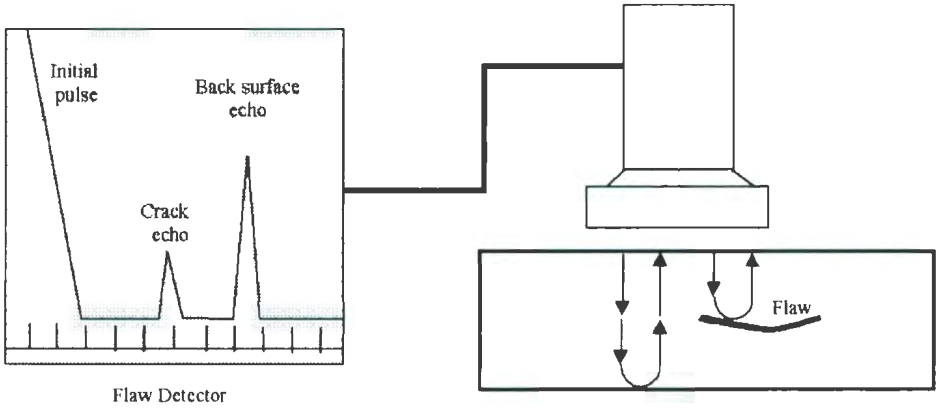

Fig. 3.15: Ultrasonic inspection technique (UI)

3.2.4.2 Advantages of Ultrasonic Inspection

Ultrasonic Inspection is a very useful and versatile NDI method. Some of the advantages of ultrasonic inspection that are often cited include:

i. It is sensitive to both surface and subsurface discontinuities.

ii. The depth of penetration for flaw detection or measurement is superior to other NDI methods.

iii. Only single-sided access is needed when the pulse-echo technique is used.

iv. It is highly accurate in determining reflector position and estimating size and shape.

v. Minimal part preparation is required.

vi. Electronic equipment provides instantaneous results.

vii. Detailed images can be produced with automated systems.

viii. It has other uses, such as thickness measurement, in addition to flaw detection.

3.2.4.3 Disadvantages of Ultrasonic Inspection

As with all NDI techniques, ultrasonic inspection also has its limitations, which include:

i. Surface must be accessible to transmit ultrasound.

ii. Skill and training is more extensive than with some other techniques.

iii. Materials that are rough, irregular in shape, very small, exceptionally thin or not homogeneous are difficult to inspect.

iv. Cast iron and other coarse grained materials are difficult to inspect due to low sound transmission and high signal noise.

v. Linear flaws oriented parallel to the sound beam may go undetected.

vi. Reference standards are required for both equipment calibration and the characterization of flaws.

3.2.5 Radiographic Inspection (RI)

3.2.5.1 Principles of Radiographic Inspection

X-rays are used to produce images of objects using film or other detector that is sensitive to radiation. The test object is placed between the radiation source and detector. The thickness and the density of the material that X-rays must penetrate affect the amount of radiation reaching the detector. This variation in radiation produces an image on the detector that often shows internal features of the test object (Fig. 3.16).

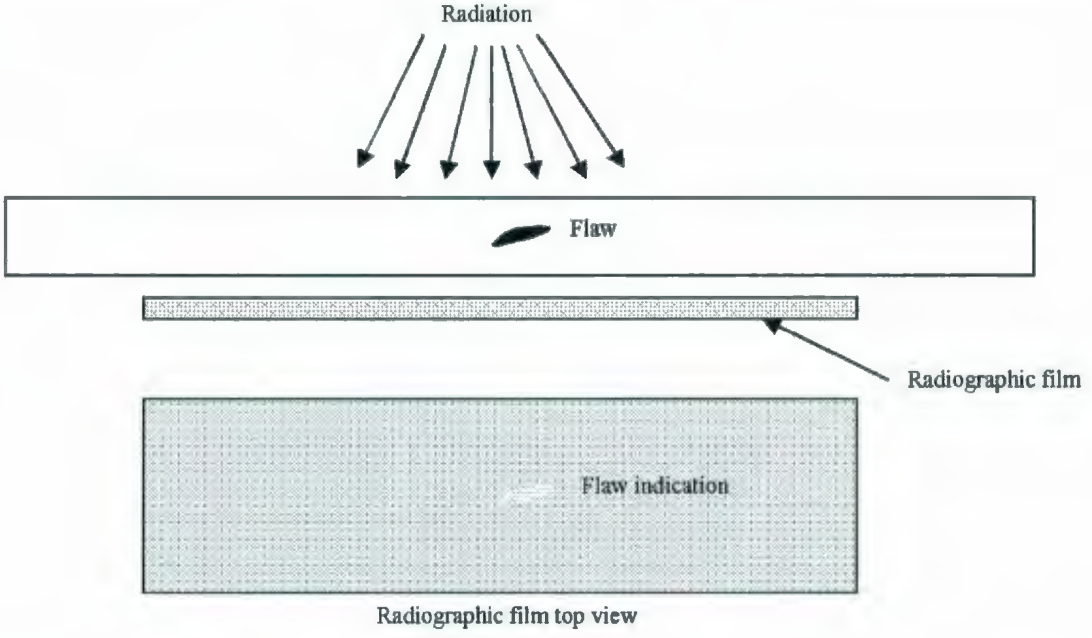

Fig. 3.16: Radiographic Inspection (RI)

3.2.5.2 Nature of Penetrating Radiation

X-rays and gamma rays differ only in their source of origin. X-rays are produced by an x-ray generator and gamma radiation is the product of radioactive atoms. They are waveforms, as are light rays, microwaves, and radio waves. X-rays and gamma rays cannot be seen, felt, or heard. They possess no charge and no mass and, therefore, are not influenced by electrical and magnetic fields and will generally travel in straight lines. However, they can be diffracted (bent) in a manner similar to light.

Both X-rays and gamma rays can be characterized by frequency, wavelength, and velocity. However, they act somewhat like a particle at times in that they occur as small "packets" of energy and are referred to as "photons". Due to their short wavelength they have more energy to pass through matter than do the other forms of energy in the electromagnetic spectrum. As they pass through matter, they are scattered and absorbed and the degree of penetration depends on the kind of matter and the energy of the rays.

3.2.5.3 Main Uses of RI

Used to inspect almost any material for surface and subsurface flaws. X-rays can also be used to locate and measure internal features, confirm the location of hidden parts in an assembly, and to measure thickness of materials.

3.2.5.4 Main Advantages of RI

i. Can be used to inspect virtually all materials.

ii. Detects surface and subsurface flaws.

iii. Ability to inspect complex shapes and multi-layered structures without disassembly.

iv. Minimum part preparation is required.

3.2.5.5 Disadvantages of RI

i. Extensive operator training and skill required.

ii. Access to both sides of the structure is usually required.

iii. Orientation of the radiation beam to non-volumetric flaws is critical.

iv. Field inspection of thick section can be time consuming.

v. Relatively expensive equipment investment is required.

vi. Possible radiation hazard for personnel.

3.2.5.6 Real-time Radiography

Real-time radiography (RTR), or real-time radioscopy, is a nondestructive inspection (NDI) method whereby an image is produced electronically, rather than on film, so that very little lag time occurs between the item being exposed to radiation and the resulting image. In most instances, the electronic image that is viewed results from the radiation passing through the object being inspected and interacting with a screen of material that fluoresces or gives off light when the interaction occurs. The fluorescent elements of the screen form the image much as the grains of silver form the image in film radiography. The image formed is a "positive image" since brighter areas on the image indicate where higher levels of transmitted radiation reached the screen. This image is the opposite of the

negative image produced in film radiography. In other words, with RTR, the lighter, brighter areas represent thinner sections or less dense sections of the inspected object.

3.2.5.7 Future Direction of Radiographic Inspection

Radiographers of the future will capture images in digitized form and e-mail them to the customer when the inspection has been completed. Film evaluation will likely be left to computers. Inspectors may capture a digitized image, feed them into a computer and wait for a printout of the image with an accept/reject report. Systems will be able to scan a part and present a three-dimensional image to the radiographer, helping in locating the flaw within the part.

3.2.6 Eddy Current Inspection (ECI)

3.2.6.1 Principles of Eddy Current Inspection

Alternating electrical current is passed through a coil producing a magnetic field (Fig. 3.17). When the coil is placed near a conductive material, the changing magnetic field induces current flow in the material. These currents travel in closed loops and are called eddy currents. Eddy currents produce their own magnetic field that can be measured and used to find flaws and characterize conductivity, permeability, and dimensional features.

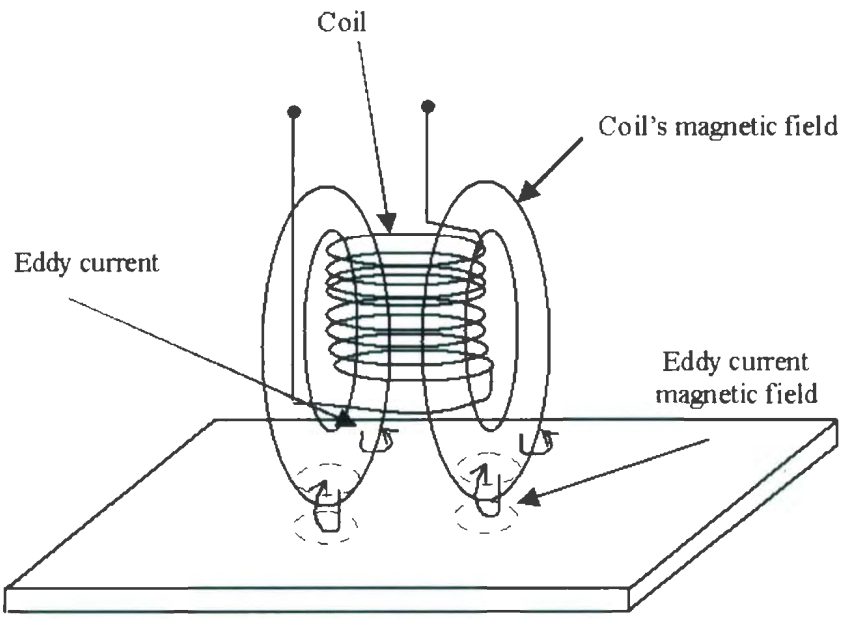

Fig. 3.17: Eddy current inspection

3.2.6.2 Main Uses of ECI

Used to detect surface and near-surface flaws in conductive materials, such as the metals. Eddy current inspection is also used to sort materials based on electrical conductivity and magnetic permeability, and measures the thickness of thin sheets of metal and nonconductive coatings such as paint.

3.2.6.3 Main Advantages of ECI

i. Detects surface and near surface flaws.

ii. Test probe does not need to contact the part.

iii. Method can be used for more than flaw detection.

iv. Minimum part preparation is required.

3.2.6.3 Disadvantages of ECI

i. Only conductive materials can be inspected.

ii. Ferromagnetic materials require special treatment to address magnetic permeability.

iii. Depth of penetration is limited.

iv. Flaws that lie parallel to the inspection probe coil winding direction can go undetected.

v. Skill and training required is more extensive than other techniques.

vi. Surface finish and roughness may interfere.

vii. Reference standards are needed for setup.

3.2.7 Acoustic Emission Inspection Technique (AEI)

3.2.7.1 Principle and Sources of AE

The AEI technique is illustrated in Fig. 3.18, It begins with forces acting on a body; the resulting stress is the stimulus (change in pressure, load, or temperature) that causes deformation and with it, acoustic emission (elastic wave that travels outward from the source, moving through the body). This wave arrives at a remote sensor. In response, the sensor produces an electrical signal, which is passed to electronic equipment for further processing.

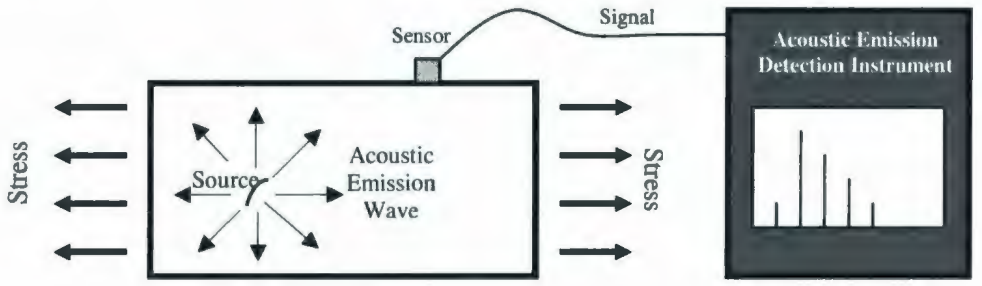

Fig. 3.18: Acoustic Emission Inspection Technique (AEI)

AE's originate with stress. When a stress is exerted on a material, a strain is induced in the material as well. The most detectible acoustic emissions take place when a loaded material undergoes plastic deformation or when a material is loaded at or near its yield stress. On the microscopic level, as plastic deformation occurs, atomic planes slip past each other through the movement of dislocations. These atomic-scale deformations release energy in the form of elastic waves which "can be thought of as naturally generated ultrasound" traveling through the object. When cracks exist in a metal, the stress levels present in front of the crack tip can be several times higher than the surrounding area. Therefore, AE activity will also be observed when the material ahead of the crack tip undergoes plastic deformation (micro-yielding).

Two sources of fatigue cracks also cause AE's. The first source is emissive particles (e.g. nonmetallic inclusions) at the origin of the crack tip. Since these particles are less ductile than the surrounding material, they tend to break more easily when the metal is strained, resulting in an AE signal. The second source is the propagation of the crack tip that occurs through the movement of dislocations and small-scale cleavage produced by triaxial stresses.

The amount of energy released by an acoustic emission and the amplitude of the waveform are related to the magnitude and velocity of the source event. The amplitude of the emission is proportional to the velocity of crack propagation and the amount of surface area created. Large, discrete crack jumps will produce larger AE signals than cracks that propagate slowly over the same distance.

Detection and conversion of these elastic waves to electrical signals is the basis of AE inspection. Analysis of these signals yield valuable information regarding the origin and importance of a discontinuity in a material.

Sources of AE vary from natural events like earthquakes and rockbursts to the initiation and growth of cracks, slip and dislocation movements, melting, twinning, and phase transformations in metals.

Acoustic Emission is unlike most other nondestructive testing (NDT) techniques in two regards. The first difference pertains to the origin of the signal. Instead of supplying energy to the object under examination, AEI simply listens for the energy released by the object. AE inspection is often performed on structures while in operation, as this provides adequate loading for propagating flaws and triggering acoustic emissions.

The second difference is that AEI deals with dynamic processes, or changes, in a material. This is particularly meaningful because only active features (e.g. crack growth) are highlighted. The ability to discern between developing and stagnant flaws is significant. However, it is possible for flaws to go undetected altogether if the loading is not high enough to cause an acoustic event. Furthermore, AE Inspection usually provides an immediate indication relating to the strength or risk of failure of a component. Other

advantages of AET include fast and complete volumetric inspection using multiple sensors, permanent sensor mounting for process control, and no need to disassemble and clean a specimen.

Unfortunately, AE systems can only qualitatively gauge how much damage is contained in a structure. In order to obtain quantitative results about size, depth, and overall acceptability of a part, other NDT methods (often ultrasonic Inspection) are necessary. Another drawback of AE stems from loud service environments which contribute extraneous noise to the signals. For successful applications, signal discrimination and noise reduction are crucial. AE can be subjected to extraneous noise. Noise in AE inspection refers to any undesirable signals detected by the sensors. Examples of these signals include frictional sources (e.g. loose bolts or movable connectors that shift when exposed to wind loads) and impact sources (e.g. rain, flying objects or wind-driven dust) in bridges. Sources of noise may also be present in applications where the area being inspected may be disturbed by mechanical vibrations (e.g. pumps).

To compensate for the effects of background noise, various procedures can be implemented. Some possible approaches involve fabricating special sensors with electronic gates for noise blocking, taking precautions to place sensors as far away as possible from noise sources, and electronic filtering.

3.2.7.2 AEI Applications

Detection and analysis of AE signals can supply valuable information regarding the origin and importance of a discontinuity in a material. Because of the versatility of acoustic emission inspection (AEI), it has many industrial applications (e.g. assessing structural

integrity, crack growth due to hydrogen embrittlement, fatigue, stress corrosion, creep, flaws detection, testing for leaks, monitoring weld quality, on-line monitoring of components and systems).

3.2.8 Thermal Inspection Technique

It is also referred as Thermography, Thermal Imaging, Thermal Wave Imaging and Infrared (IR) Inspection. Thermal NDI technique involves the measurement or mapping of surface temperatures as heat flows to, from and/or through an object. The simplest thermal measurements involve making point measurements with a thermocouple. This type of measurement might be useful in locating hot spots, such as a bearing that is wearing out and starting to heat up due to an increase in friction or locating hot spots in fired heater casing due to damage in the refractory.

In its more advanced form, the use of thermal imaging systems allow thermal information to be very rapidly collected over a wide area and in a non-contact mode. Thermal imaging systems are instruments that create pictures of heat flow rather than of light. Thermal imaging is a fast, cost effective way to perform detailed thermal analysis.

The basic premise of thermographic NDI is that the flow of heat from the surface of a solid is affected by internal flaws such as voids or inclusions.

3.2.8.1 Principles of Thermal Inspection

Thermal energy transfer occurs through three mechanisms: conduction, convection, and/or radiation. Conduction occurs primarily in solids and to a lesser degree in fluids as warmer, more energetic molecules transfer their energy to cooler adjacent molecules.

Convection occurs in liquids and gases, and involves the mass movement of molecules such as when stirring or mixing is involved.

The third way that heat is transferred is through electromagnetic radiation of energy. Radiation needs no medium to flow through and, therefore, can occur even in a vacuum. Electromagnetic radiation is produced when electrons lose energy and fall to a lower energy state. Both the wavelength and intensity of the radiation is directly related to the temperature of the surface molecules or atoms.

The wavelength of thermal radiation extends from 0.1 microns to several hundred microns. Not all of the heat radiated from an object will be visible to the human eye, but the heat is detectable. Consider the gradual heating of a piece of steel. With the application of a heat source, heat radiating from the part is felt long before a change in color is noticed. If the heat intensity is great enough and applied for long enough, the part will gradually change to a red color. The heat that is felt prior to the part changing color is the radiation that lies in the infrared frequency spectrum of electromagnetic radiation. Infrared (IR) radiation has a wavelength that is longer than visible light or (greater than 700 nanometers). As the wavelength of the radiation shortens, it reaches the point where it is short enough to enter and be visible with the human eye.

Some thermal imaging techniques simply involve pointing a camera at a component and looking at areas of uneven heating or localized hot spots. For some other applications, it may be necessary to generate heat flow within the component and/or evaluate heat flow as a function of time.

An infrared camera has the ability to detect and display infrared energy. The basis for infrared imaging technology is that any object whose temperature is above 0°K radiates infrared energy.

3.2.8.2 Applications of Thermal Imaging

i. Electrical and Mechanical System Inspection

Electrical and mechanical systems are the backbone of many manufacturing operations. An unexpected shutdown of even a minor piece of equipment could have a major impact on production. Since nearly everything gets hot before it fails, thermal inspection is a valuable and cost-effective diagnostic tool with many industrial applications. With the infrared camera, an inspector can see the change in temperature from the surrounding area, identify whether or not it is abnormal and predict the possible failure. Applications for infrared testing include locating loose electrical connections, failing transformers, improper bushing and bearing lubrication, overloaded motors or pumps, coupling misalignment, and other applications where a change in temperature will indicate an undesirable condition.

ii. Corrosion Damage (Metal Thinning)

IR techniques can be used to detect material thinning of relatively thin structures since areas with different thermal masses will absorb and radiate heat at different rates. In relatively thin, thermally conductive materials, heat will be conducted away from the surface faster by thicker regions. By heating the surface and monitoring its cooling characteristics, a thickness map can be produced (Fig.

3.19). Thin areas may be the result of corrosion damage on the backside of a structure which is normally not visible.

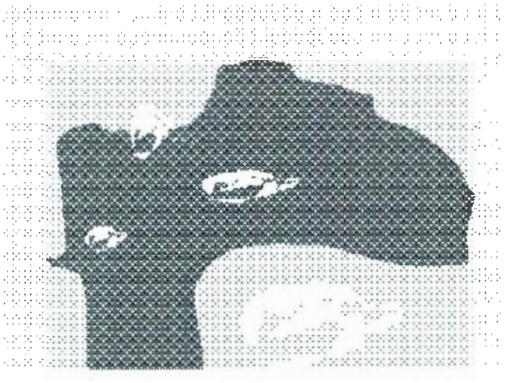

Fig. 3.19: Metal thinning detection using IR inspection technique

iii. Flaw Detection

Infrared techniques can be used to detect flaws in materials or structures. The inspection technique monitors the flow of heat from the surface of a solid and this flow is affected by internal flaws such as voids or inclusions. Sound material, a good weld, or a solid bond will see heat dissipate rapidly through the material, whereas a flaw will retain the heat for longer. The inspected component can be directly heated or alternatively excited (using vibrothermograph or thermosonic) with bursts of high-energy, low-frequency acoustic energy. This causes frictional heating at the faces of any cracks present and hotspots are detected by an infrared camera, Fig. (3.20).

Fig. 3.20: Flaw detection using IR inspection technique

iv. Stress concentration detection

Stress concentration or areas of high fatigue show up as hot spots in IR scans because the higher temperature or the stressed areas.

3.2.8.3 Main Advantages of Thermal Inspection

i. Fast data acquisition

ii. Minimal surface preparation

iii. No contact needed and works good in complex geometry to avoid high cost of disassembly

iv. Portable

3.2.8.4 Main Disadvantages of Thermal Inspection

i. High first cost

ii. Structures to be fatigued or heated for thermal activity

iii. Only surface stress is obtainable not internal stress

3.3 Buried Pipeline Inspection

Engineers have developed devices, called pigs, that are sent through the buried pipe to perform inspections and clean the pipe. The pigs are carried through the pipe by the flow of the liquid or gas and can travel and perform inspections over very large distances. They may be put into the pipe line on one end and taken out at the other. The pigs carry a small computer to collect, store and transmit the data for analysis. In 1997, a pig set a world record when it completed a continuous inspection of the Trans Alaska crude oil pipeline, covering a distance of 1,055 km in one run.

Pigs use several nondestructive testing methods to perform the inspections. Most pigs use a magnetic flux leakage method but some also use ultrasound to perform the inspections. For example, the pig shown in Fig. 3.21 uses magnetic flux leakage.

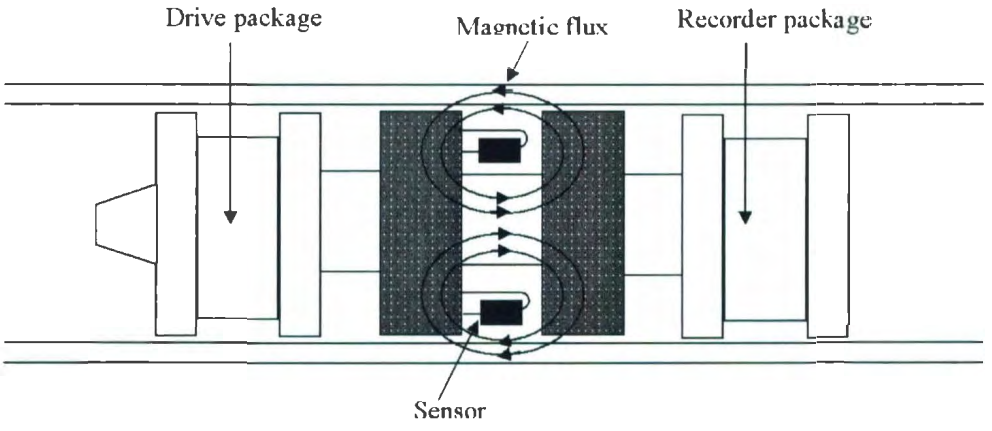

Fig. 3.21: A pig uses magnetic flux leakage technique for buried pipe line inspection

On some pipelines it is easier to use remote visual inspection equipment to assess the condition of the pipe. Robotic crawlers of all shapes and sizes have been developed to

navigate the pipe. The video signal is typically fed to a truck where an operator reviews the images and controls the robot.

Chapter 4

Crack Growth Assessment

Subcritical crack growth can occur prior to reaching the critical crack size. This can occur due to fatigue, corrosion, creep or combination between two or more of these degradation mechanisms (e.g., corrosion fatigue, creep-fatigue interaction).

The ability of the NDI technique to detect a crack is a function of the crack size and therefore assessment of the crack size is required when selecting an optimal NDI technique.

4.1 Fatigue Cracking

4.1.1 Fatigue Crack Growth Rate

Fatigue crack growth can be modeled using the well known Paris Law (1963) which relates crack growth to the number of stress cycles as follows:

$$\frac{da}{dN} = C.(\Delta k)^m \tag{4.1}$$

Where a is the crack size, N is the number of stress cycles, C and m are material constants for fatigue crack growth and Δk is the stress intensity range factor which, in general, can be calculated as follows:

$$\Delta k = F(a).\Delta\sigma.\sqrt{\pi a} \tag{4.2}$$

Where $\Delta\sigma$ is the applied stress range and F(a) is the geometry function.

In logarithmic coordinates, the Paris equation is represented by the straight line (AB) as shown in Fig 4.1.

In practical applications, the linear relationship between (lnda/dN) and ($\ln\Delta k$) could be extrapolated up to the threshold stress intensity range, Δk_{th} (point C) while Δk_{th} is the stress intensity range at which the crack begins to propagate. This extrapolation will give overestimate to the crack growth rate in the vicinity of Δk_{th} (portion AC). The critical stress intensity range Δk_{cr} is smaller than the fracture toughness Δk_f and located on the straight line AB.

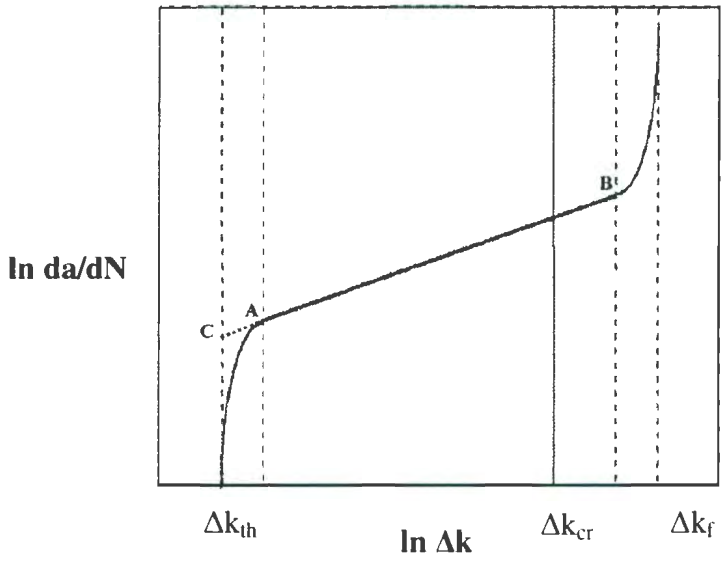

Fig. 4.1: Typical fatigue crack growth

An integral form of Paris Law is given by

$$N = \int_{a_o}^{a_N} \frac{da}{C[\Delta\sigma.F(a).\sqrt{\Pi a}]^m} \tag{4.3}$$

Where a_o is the initial crack size; a_N is crack size after N stress cycles. The geometry function, F(a), for a specific fatigue component may be obtained from the available stress intensity manuals or derived using fracture mechanics principles.

The geometry function depends on the geometry of the body (e.g., plate, pipe), location of the crack (e.g., edge, center, distributed) and loading (e.g., normal load, bending).

Analytical integration of Paris Law is not possible in most applications since the geometry functions are not mathematically simple. For simplicity consider the case of a loaded plate where F(a) does not much change within the range a_o to critical size, a_{cr}, a

weighted average geometry function, $F_{av} = [F(a_o) + F(a_{cr})]/2$ may be used [Ragab and Bayoumi (1999)]; hence integration of Paris Law yields:

For m = 2:

$$N_{cr} = \frac{\ln(a_{cr}/a_o)}{C\Pi[\Delta\sigma.F_{av}(a)]^2} \tag{4.4}$$

For $m \neq 2$:

$$N_{cr} = \frac{a_{cr}^{(1-\frac{m}{2})} - a_0^{(1-\frac{m}{2})}}{C.[F_{av}]^m \Pi^{\frac{m}{2}}.(\Delta\sigma)^m[1-\frac{m}{2}]} \tag{4.5}$$

Where N_{cr} is the critical number of stress cycles and a_{cr} is the critical crack size.

$N_{cr} = f.\ t_{cr}$ where f is frequency of loading (e.g. 500,000 cycle/year) and t_{cr} is the critical time to failure.

Harris (1992) provides a review of probabilistic fracture mechanics and gives examples from reported literatures for fatigue crack growth for some materials (e.g., Inconell 718 at 70° F in hydrogen, Inconell 718 at 70° F in air, $2^1/_4$ Cr-1Mo steel at 1000° F). This review shows that Paris equation gives a good fit to fatigue crack growth rate for $2^1/_4$ Cr-1Mo steel at 1000° F in air, with m = 2.87 and $C = 6.607 \times 10^{-10}$ (da/dN in inches per cycle and ΔK in ksi-$in^{1/2}$).

Flaws detected by the pre-service and in-service inspections may be planar or volumetric and located on surface or subsurface. ASME Boiler and pressure vessels code, section XI, provides the rules for approximating the initial crack size, a_o, based on flaw shape,

proximity to closest flaw, flaw orientation, and flaw location, which are used in the analytical model for linear elastic fracture mechanics.

Theses volumetric flaws and planar flaws may initiate cracks after number of stress cycles. As a conservative procedure volumetric flaws and planar flaws can be considered as cracks with initial size as the initial size of theses flaws [ASME, section XI] neglecting the time for initiating a fatigue crack from a flaw in comparison with fatigue life.

In practical engineering applications, surface and embedded cracks usually have an irregular shape. Δk depends on crack size as well as crack shape. Crack shape can have a significant influence on crack growth rates and accumulated crack growth. In principal, changes in crack shape as well as crack size could be tracked by predicting the incremental crack growth at various locations along the crack front. However, such an approach is time-consuming and impractical. Usually, an embedded flaw is characterized as an elliptic crack, and crack growth is only predicted along the major and minor axes of the idealized flaw. Similarly, a surface flaw is characterized as a semi-elliptic crack, and growth is only predicted at the deepest point and surface [ASME, section XI].

4.1.2 Effective Stress Range

To account for the variable amplitude stress ranges that result from random stress range, $\Delta\sigma$, can be replaced by an effective constant stress range, $\Delta\sigma_{eff}$, which represents a weighted effect of stress ranges of all amplitudes and produces the same crack growth rate.

Schilling et al. (1978) proposed the use of the root mean cube (RMC) of the collected stress range spectrum in a component as the effective stress range, $\Delta\sigma_{eff}$, for fatigue evaluation:

$$\Delta\sigma_{eff} = \left[\sum_{i=1}^{n} R_i.(\Delta\sigma_i)^3\right]^{\frac{1}{3}} \tag{4.6}$$

Where R_i = ratio of the number of cycles with ith stress range amplitude, $\Delta\sigma_i$, to the total number of cycles (a total of n ranges are considered).

Another method for calculating $\Delta\sigma_{eff}$ is to use the following equation [Ship Structure Committee, SSC (1997)]:

$$\Delta\sigma_{eff} = \left[\sum_{i=1}^{n} R_i.(\Delta\sigma_i)^m\right]^{\frac{1}{m}} \tag{4.7}$$

Where m is material exponent for crack growth rate.

Some studies have shown that the stress range, $\Delta\sigma$, spectrum may be modeled by Rayleigh distribution [Schilling et al. (19780] or Weibull distribution [Cramer et al. (1995)]. Rayleigh distribution is usually applied to define narrow banded stress spectrum and Weibull distribution is usually applied to define long banded stress spectrum. For Rayleigh distribution, the effective stress range, $\Delta\sigma_{eff}$, can be expressed in terms of gamma function, $\Gamma(\ )$, [Chung et al. (2006)] as follows:

$$\Delta\sigma_{eff} = \{E[\Delta\sigma^m]\}^{\frac{1}{m}} \tag{4.8}$$

$$\Delta\sigma_{eff\text{-Rayleigh}} = \{E[\Delta\sigma^m]\}^{\frac{1}{m}} = \sqrt{2}.b.\Gamma(1+\frac{m}{2})^{\frac{1}{m}} \tag{4.9}$$

Where b is parameter of Rayleigh distribution, $E[\Delta\sigma^m]$ is mean of $\Delta\sigma^m$.

For Weibull distribution, $E[\Delta\sigma^m]$ can be calculated as follows [Cramer et al. (1992)]:

$$E[\Delta\sigma^m] = \theta^m.\Gamma(1+\frac{m}{\beta}) \tag{4.10}$$

Where θ and β are scale and shape parameter of Weibull distribution respectively.

Equations 4.8 and 4.10 lead to the effective stress for Weibull distribution as follows:

$$\Delta\sigma_{eff,\text{Weibull}} = \{E[\Delta\sigma^m]\}^{\frac{1}{m}} = \theta.\Gamma(1+\frac{m}{\beta})^{\frac{1}{m}} \tag{4.11}$$

The Rayleigh distribution is a special case of the Weibull distribution where Rayleigh distribution with parameter b is equivalent to the Weibull distribution with parameters $\theta = \sqrt{2}.b$ and $\beta = 2$.

4.2 Crack Growth Due to Stress Corrosion Cracking (SCC)

Crack growth due to SCC is a function of the material condition, environment, the stress intensity factor due to sustained loading, and the total time that the flaw is exposed to the environment under sustained loading. ASME code, section XI gives procedure for computing SCC crack growth based on experimental data relating the flaw growth rate (da/dt) to the sustained load stress intensity factor K. The procedure used for determining the cumulative crack growth is as follows [ASME code, section XI]

(1) Determine the stress intensity factor K for a given steady state stress condition.

(2) Calculate the incremental growth of the crack size corresponding to the period for which the steady state stress is applied. This can be obtained from the relationship

between da/dt and K. A sufficiently small time interval shall be selected to ensure that the crack size and the associated K value do not change significantly during this interval.

(3) Update the crack size.

(4) Continue the crack growth analysis for the period during which the stress exists until the end of the evaluation period.

The above procedure yields the final crack size at the end of the evaluation period, considering SCC crack growth alone.

The crack growth rate for alloy 600 in primary water reactor (PWR) environments can be given by the following equation [ASME code, section XI]:

$$\frac{da}{dt} = \exp\left[-\frac{Q_g}{R}\left(\frac{1}{T}-\frac{1}{T_{ref}}\right)\right]\alpha\left(K - K_{th}\right)^{\beta} \quad , K>K_{th} \qquad (4.12)$$

Where

da/dt = crack growth rate at temperature T in m/s

Q_g = thermal activation energy for crack growth = 130 kJ/mole

R = universal gas constant = 8.314 x 10^{-3} kJ/mole °K

T = absolute operating temperature at location of crack, °K

T_{ref} = absolute reference temperature used to normalize data = 598.15 °K

α = crack growth rate coefficient = 2.67 x 10^{-12} at 325°C for da/dt in units of m/s and K in units of MPa .$m^{1/2}$

K = crack tip stress intensity factor, MPa .$m^{1/2}$

K_{th} = crack tip stress intensity factor threshold for SCC = 9 MPa .$m^{1/2}$

β = exponent = 1.16

When K is less than or equal to K_{th} and da/dt = 0.

White, et. al, (2005) reported the results of work sponsored by the Electric Power Research Institute (EPRI) Materials Reliability Program (MRP) to develop crack growth rate curves for primary water stress corrosion cracking (PWSCC) of alloy 82, 182 and 132 weld metal at different temperatures, conservatively assuming no stress intensity factor threshold for PWSCC (i.e., K_{th} = 0). The general form of MRP equation is as follows:

$$\frac{da}{dt} = \exp\left[-\frac{Q_g}{R}\left(\frac{1}{T}-\frac{1}{T_{ref}}\right)\right]\alpha . f_{alloy} . f_{orient} K^{\beta} \qquad (4.\ 13)$$

Where:

da/dt, Q_g, R, T, T_{ref} and K are as defined in the ASME-Section XI equation

α = power-law constant

= 1.5 x 10^{-12} at 325°C for da/dt in units of m/s and K in units of MPa .$m^{1/2}$

f_{alloy} = 1.0 for Alloy 182 or 132 and 1/206=0.385 for Alloy 82

f_{orient} = 1.0 except 0.5 for crack propagation that is clearly perpendicular to the dendrite solidification direction

β = exponent

= 1.6

The form of the MRP equation at 325°C is as follows:

For Alloy 182 and 132:

$$\frac{da}{dt} = 1.5x10^{-12} K^{1.6} \qquad (4.14)$$

For Alloy 82:

$$\frac{da}{dt} = (1.5x10^{-12} / 2.6).K^{1.6} \qquad (4.15)$$

4.3 Crack Growth Due to a Combination of Fatigue and SCC

When the service loading and environmental conditions are such that the crack is subjected to both fatigue and SCC growth, the final crack size are obtained by adding the increments in crack size due to fatigue and SCC [ASME, Section XI].

In a real application, a better fit to crack growth data generated under simulated operating conditions and environments would be needed.

Chapter 5

Optimization Model

This chapter proposes a new methodology for selecting an optimal non-destructive inspection technique and its associated optimum inspection interval for welded component.

5.1 Reliability of the NDI Techniques

The most common NDI techniques are the ultrasonic inspection (UI), the magnetic particle inspection (MI), the penetrant inspection (PI), the radiographic inspection (RI), the eddy current inspection (ECI), and the visual inspection (VI). Two main parameters are used to quantify the reliability of NDI techniques. These are the Probability of Detection function (POD) and the Probability of False Calls, (PFC).

The POD function is a measure of the ability of the technique to detect an existing flaw. It is a function of the flaw size, a. The following procedure can be followed to determine an estimate for the POD function for a specific NDI technique. First, a number of flaws with various sizes are either artificially introduced in a number of test specimens or are

existing as a pre-service flaws or in-service flaws [Faher, et al. (1995)]. A specific NDI technique is used to detect these flaws. The ratio of the number of flaws detected to the number of the flaws actually existing is calculated. After the completion of the inspection of all samples, the samples are sectioned destructively to verify the presence of the flaws and to measure their sizes. The POD curve obtained is discrete. Each point is representative of a crack class range, and the probability of detection in that class is the number of actual detected cracks divided by the total number of actual cracks in that class.

Berens and Hovey (1981) suggested using the log-odds or log-logistic model for expressing the POD function as follows:

$$POD(a) = \frac{\exp(\alpha + \beta.\ln a)}{1 + \exp(\alpha + \beta.\ln a)} \tag{5.1}$$

Where a is the crack size in mm, α and β are experimentally determined parameters.

Staat (1993) suggested that POD can be formulated as follows:

$$POD(a) = (1-p)\,(1-\exp(-ca)) \quad ; \quad a \geq 0 \tag{5.2}$$

Where c is a parameter derived from experimental data and p is the asymptotic non detection probability for large values of a (i.e. $a \rightarrow \infty$). Typical values for p are of the order of 0.01-0.05 for flaw sizes of practical interest.

PFC is defined as the fraction of times that unflawed component will be incorrectly classified as being flawed. False calls could lead to costly repair that is actually not required as the flaw does not actually exist.

Heasler et al. (1993) proposed a model for POD function includes probability of false calls as follows:

$$POD(a) = (1+\exp(-(A+Ba)))^{-1} \quad (5.3)$$

From Eq. 5.3, by comparing the definitions of POD and PFC, it can be seen that PFC is the value of POD at flaw size a = 0. Hence PFC can be obtained as follows:

$$PFC = POD(0) = (1+\exp(-A))^{-1} \quad (5.4)$$

Where A and B are parameters regressed from experimental data.

5.2 Condition of the Inspected Component

Condition of the inspected component can be expressed by two parameters as follows:

i. The critical time to failure (t_{cr}) at which the growing fatigue crack reaches the critical size, a_{cr}.

ii. Probability of presence of a crack in the inspected component (H) which can be calculated as follows:

$$H_i = \int_0^{a_i} f_i(a)\, da \quad (5.5)$$

Where H_i is probability of presence of a crack in the inspected asset at the time of the ith inspection

a_i and $f_i(a)$ are crack size and probability density function of the crack size, a, at time of the ith inspection, respectively.

5.3 The Proposed Optimization Model

The crack size, a, is obtained as a function of the applied effective stress range ($\Delta\sigma_{eff}$), stress frequency (f), the material parameters for fatigue crack growth (C and m) and the intial crack size, a_o. The critical time to failure (t_{cr}) is obtained as a function of the effective stress range ($\Delta\sigma_{eff}$), stress frequency (f), the critical size (a_{cr}), the initial crack size (a_o) and the material parameters for fatigue crack growth (C and m). The applied variable stress range ($\Delta\sigma$) is replaced by a constant effective stress range ($\Delta\sigma_{eff}$). The applied variable stress range ($\Delta\sigma$), material parameters (C and m) and initial crack size, a_o are in general random variables. In order to consider all possible combinations of these random variables, Monte Carlo method is applied to simulate the crack growth rate in order to obtain the crack size (a), using Paris law [Paris and Erdogan (1963)], as a function of time (t) then POD of crack size at time of ith inspection, POD(a_i), can be obtained from POD function (Eq. 5.1) and probability of presence of a crack in the inspected detail at time of the ith inspection (H_i) can be obtained from Eq. 5.5.

The objective function, OF, is obtained for a given NDI technique as a function of reliability of the NDI technique (POD and PFC), condition of the inspected component (t_{cr} and H) and the inspection interval (t_{int}). The decision variables (controllable) are PFC, POD and t_{int}. The objective function is subject to the safety constraint that probability of failure to detect a growing crack before reaching the critical size, E[P_f], does not exceed a predefined level, $P_{f,accept}$.

The optimization problem can be summarized as follows:

Minimize $OF = OF\left(POD(a), PFC, H(a), t_{cr}(a_o, a_{cr}, C, m, \Delta\sigma_{eff}, f), t_{\text{int}}\right)$

Subject to:

$E[P_f] < P_{f,accept}$

By considering all the candidate NDI techniques, the minimum value of the objective function for each technique can be compared so as to finally lead to the optimal selection of NDI technique and associated inspection interval. The proposed optimization model is illustrated in the following flowchart, Fig 5.1.

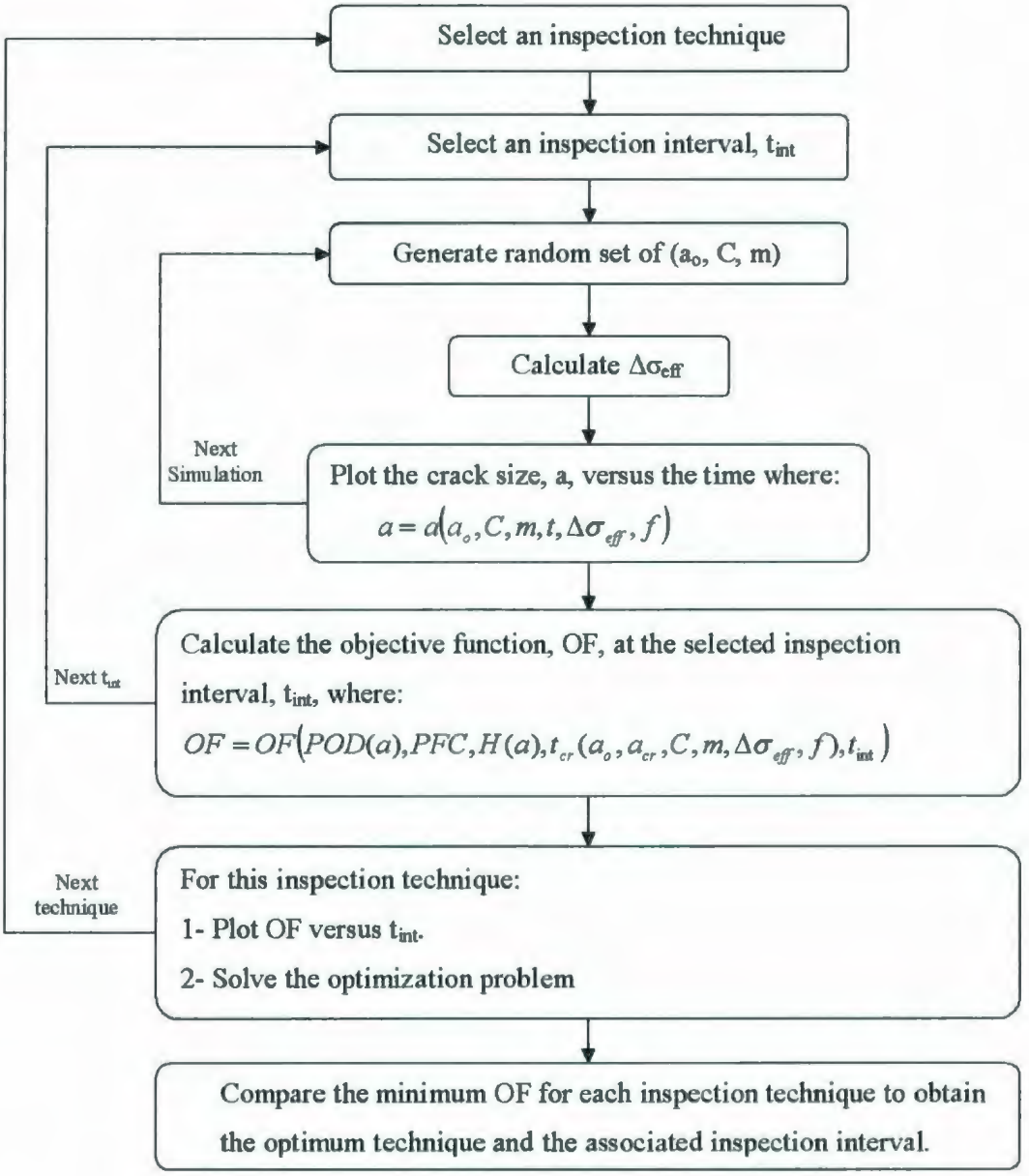

Fig. 5.1: Optimization Model Flowchart

5.4 Simulation of the Crack Size as a Function of Time

The crack growth rate depends on the variables (initial crack size, a_o, crack growth parameter, C, crack growth exponent, m, and the stress range, $\Delta\sigma$). Previous studies have

shown that a_o may be modeled by a Wiebull, Exponential or Lognormal distribution [Moan et al. (1997) and Thurlbeck et al. (1996)]. Crack growth parameter, C, and crack growth exponent, m, may be modeled using lognormal and normal distribution respectively [Tanaka et al. (1981)]. The stress range, $\Delta\sigma$, may be modeled using Rayliegh or Weibull distribution. By applying a sufficient number of simulations to the crack growth curve, all possible combinations of these random variables can be considered to take into account all possible crack growth rates. In each possible crack growth rate, the crack will reach its critical crack size at a time, t_{cr} [i.e, $a_{cr} = a(t_{cr})$].

Time to failure, t_{cr}, in a single simulation may be either longer or shorter than the time, t_1, when the first inspection is performed [Chung et al. (2006)] as shown in Fig. 5.2.

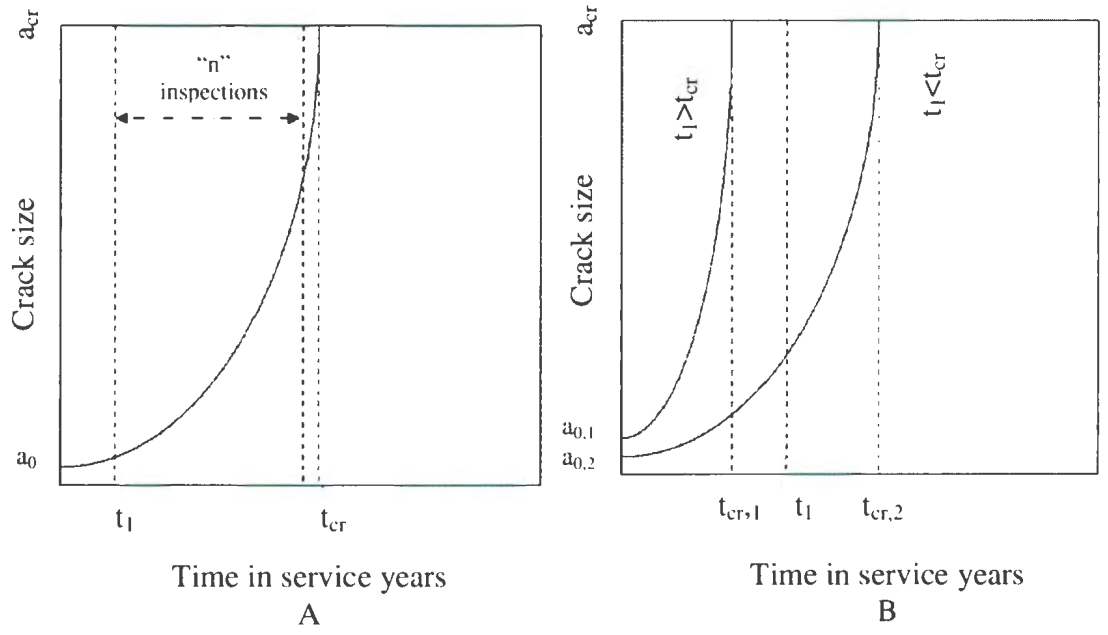

Fig. 5.2: Simulation of crack size as a function of time

(A, one simulation and B, two simulations)

5.5 Crack Size Distribution

The initial distribution of the sizes of existing cracks can be obtained from pre-service inspection. After putting the component into service, the cracks grow with time under fatigue. An approach suggested for estimating the mean, the standard deviation and the probability density function for the crack size at the inspection time is illustrated in Fig. 5.3.

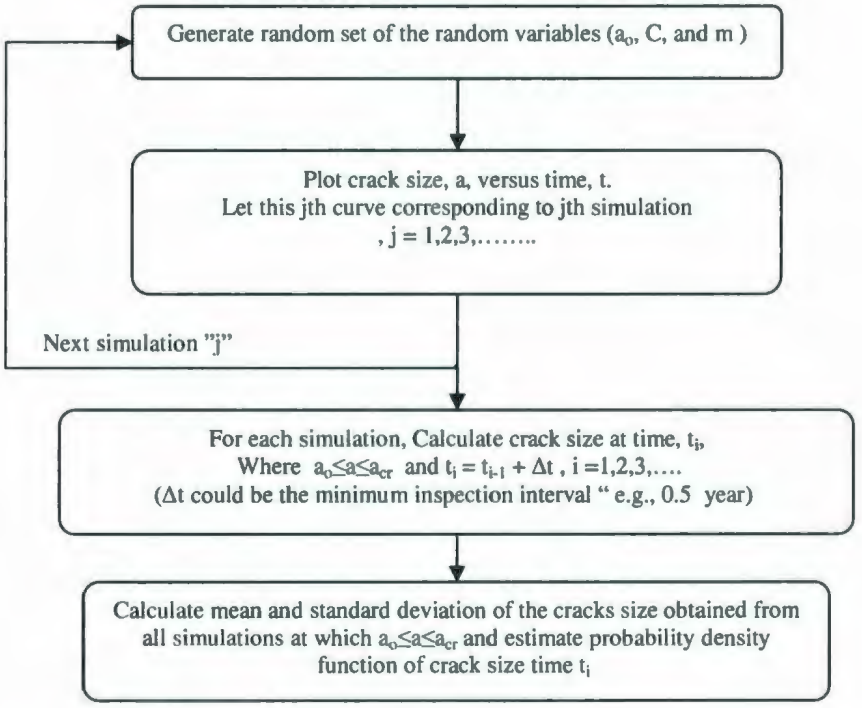

Fig. 5.3: Distribution of crack size at the inspection time

5.6 Possible Inspection Outcomes

The inspected asset could have one of two states: crack or no crack. The inspection technique can produce a positive or negative result. The combinations of these four states can result in one of the following events:

Event E_1: The asset is not cracked and the inspection result is negative. In this case no action needs to be taken.

Event E_2: The asset has no crack and the inspection result is positive. This is a case of false call. An unnecessary repair action may be carried out which will lead to additional cost.

Event E_3: The asset is cracked but the inspection result is negative. This is a case of misdetection which can lead to failure if the crack is larger than the critical size.

Event E4: The asset is cracked and the inspection result is positive. This is a case of good detection and a repair decision will be made in this case.

The four possible inspection outcomes are indicated in Table 5.1.

Table 5.1: Possible outcomes from any inspection technique

Asset's state	Inspection result	
	Negative result (no crack detected)	Positive result (crack detected)
No crack	E_1	E_2
Crack exists	E_3	E_4

Let **d** = Event of detecting a crack and h = Event of a crack existing in the inspected area. The probability of detection (POD) is defined as the conditional probability that the

inspection technique will produce a positive result given that the asset has an existing crack. The probability of false calls (PFC), is defined as the conditional probability that the inspection technique will produce a positive result given that the asset does not have an existing crack. The probabilities POD and PFC can be expressed as:

$$POD = P(d \mid h) \tag{5.6}$$

$$PFC = P(d \mid h') \tag{5.7}$$

Fig. 5.4 shows the event tree of the inspection outcomes.

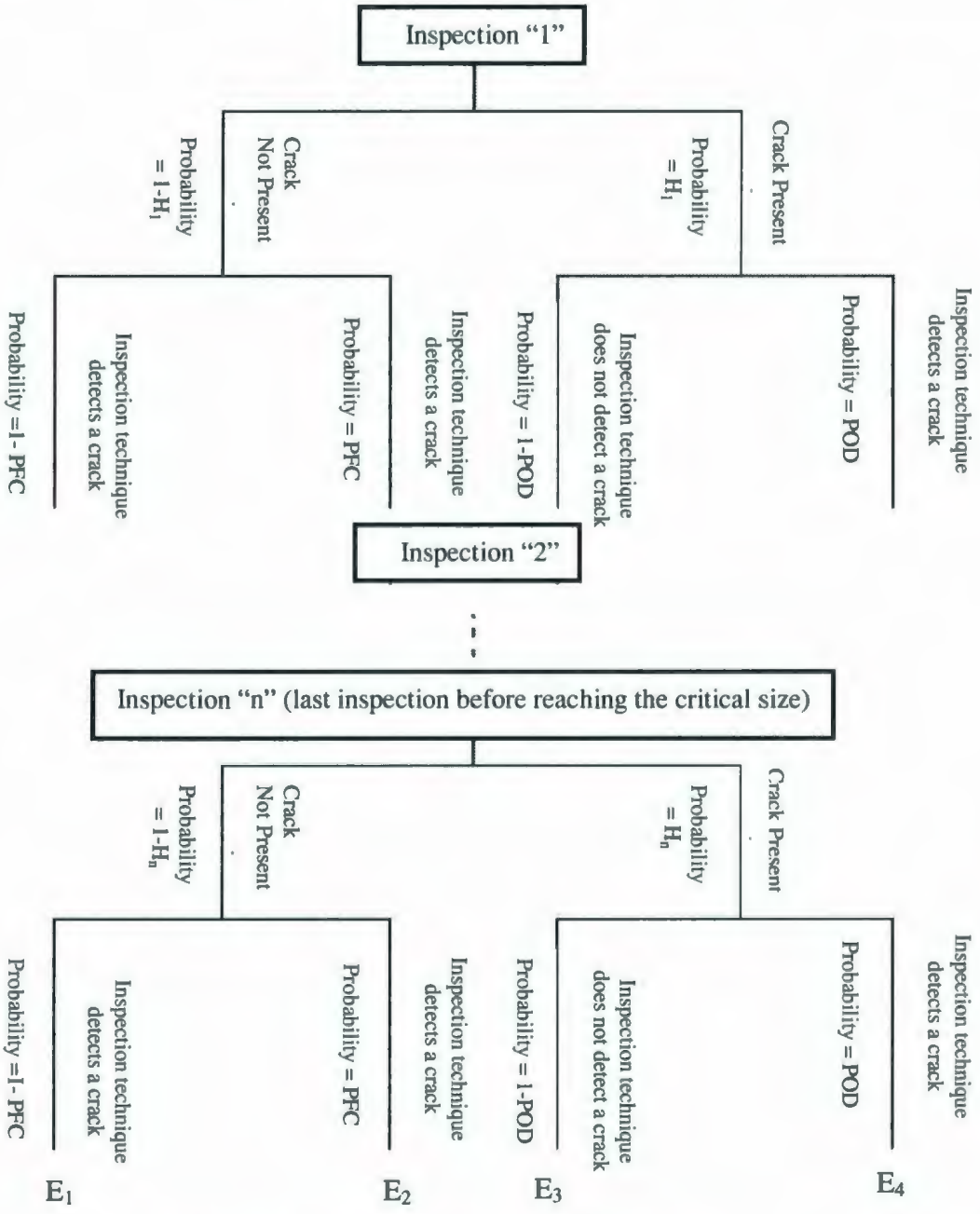

Fig. 5.4: Event tree of the inspection outcomes

The probability of occurrence for each event at ith inspection can be estimated using the event tree as follows:

$$P(E_1) = (1-H_i).(1-PFC) \tag{5.8}$$

$$P(E_2) = (1-H_i).(PFC) \quad (5.9)$$

$$P(E_3) = (H_i).(1-POD_i) \quad (5.10)$$

$$P(E_4) = (H_i).(POD_i) \quad (5.11)$$

Where $H_i=H(a_i)$ and $POD_i=POD(a_i)$ are the probabilities that the asset has an existing crack and probability of detection function at the ith inspection, respectively, where at ith inspection the crack size, $a, = a_i$.

5.7 Repair Probability

When the result of an inspection is positive (events E_2 and E_4), an acceptance or repair decision of the detected crack will be made based on a comparison between the size of a detected crack and the maximum acceptable crack size, a_r. A repair will be undertaken if the detected crack is not accepted. In case of event E_2, the undertaken repair is false repair but in case of event E_4, the undertaken repair is justifiable repair.

Let A_i = probability of acceptance of crack with size a_i at the ith inspection = $P(a_i<a_r)$.

From decision tree shown in Fig. 5.5, probability of justifiable repair at ith inspection, $P_i(JR)$, can be estimated from the following equation:

$$P_i(JR)= P(E_4).(1-A_i) = (H_i).(POD_i).(1-A_i) \quad (5.12)$$

The crack growth rate is simulated using Monte Carlo method, a_i can be estimated at time of ith inspection for each simulation. Hence, in one simulation, $A_i = 1$ if $a_i \leq a_r$ and $A_i = 0$ if $a_i>a_r$.

The inspection technique could give false calls greater or less than a_r. To take that into account:

Let the size of the flaw which is indicated by the inspection technique while actually the crack does not exist = a_f (false calls as actually "a = 0").

Let $F = P(a_f > a_r)$, where F can be estimated from the following equation..

$$F = 1 - \int_0^{a_r} f(a_f) da_f \tag{5.13}$$

$f(a_f)$ is probability density function of the cracks size indicated as false calls (incorrectly indicated by the inspection technique while actually no crack exists). From repair decision tree, probability of false repair at the ith inspection, $P_i(FR)$, can be estimated as follows:

$$P_i(FR) = P(E_2).F = (1-H_i).(PFC).\ F \tag{5.14}$$

As a special case, in some critical applications, the repair policy dictates that repairs will be undertaken when the inspection result is positive indicating any crack size (i.e. the maximum acceptable crack size, $a_r = 0$). In this special case:

$$F = P(a_f > a_r) = P(a_f > 0) = 1 - \int_0^{a_r=0} f(a_f) da_f = 1 \tag{5.15}$$

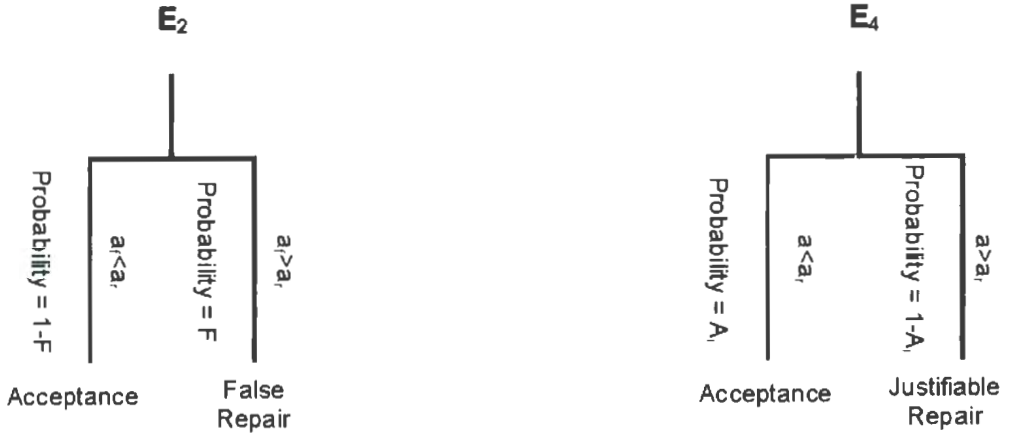

Fig. 5.5: Repair Decision Tree

5.8 Formulation of the Objective Function

The optimization problem is to determine the decision variables (PFC, POD and inspection interval) giving the minimum value of the objective function (total cost) subject to the safety constraint that probability of failure as a result of nondetection a growing crack before reaching the critical size does not exceed a predefined level. Determination of the two decision variables (PFC and POD) means selection of the optimum NDI technique while determination of the third decision variable (inspection interval) means selection of the optimum inspection interval.

The objective function, OF, may be defined as follows:

$$OF = E[C_I] + E[C_R] + E[C_f] \tag{5.9}$$

Where

, $E[C_I]$ = Expected cost of inspections over the lifetime.

, $E[C_R]$ = Expected cost of repairs over the lifetime.

, $E[C_f]$ = Expected cost of failure

The expected cost of inspections during the lifetime of the asset, $E[C_I]$, can be estimated as follows:

$$E[C_I] = E[n] \cdot K_I \tag{5.10}$$

Where $E[n]$ is the expected number of inspections over the lifetime prior to reaching the crack size to the critical size and K_I = Cost of one inspection.

Consider a situation where n nondestructive inspections are performed on a component at a constant inspection interval, t_{int}. The expected number of inspections during the lifetime of the inspected component can be estimated as follows [Chung et al. (2006)]:

$$E[n] = E[n|\, t_I \le t_{cr}].P(t_I \le t_{cr}) + E[n|\, t_I > t_{cr}].P(t_I > t_{cr}) \tag{5.11}$$

Where t_I is time to the first inspection and t_{cr} is critical time to failure.

$$\Rightarrow E[n] = \left(\frac{\sum_{j=1}^{N_1} n_j}{N_1} \right) \cdot \left(\frac{N_1}{N} \right) + (0) \cdot \left(\frac{N_2}{N} \right) = \frac{\sum_{j=1}^{N_1} n_j}{N} \tag{5.12}$$

Where N is total number of simulations and N_1 is number of simulations at which the first inspection time, t_I, is less than or equal the critical time and N_2 is number of simulations at which the first inspection time is more than the critical time while, in this case, there will be no inspections and no repair decisions will be made. n_j is number of inspections in simulation number "j". n_j can be calculated as follows:

$$n_j = Integer\left(\frac{t_{cr,j}}{t_{int}}\right) \tag{5.13}$$

Where $t_{cr,j}$ is the critical time (time to reaching the crack size to the critical size, a_{cr}) in jth simulation.

E[n] can also be estimated as follows:

$$E[n] = \frac{\text{Mean time to failure}}{\text{Inspection interval}} = \frac{\left(\frac{\sum_{j=1}^{N} t_{cr,j}}{N}\right)}{t_{int}} \tag{5.14}$$

The expected cost of failure, $E[C_f]$, corresponding to event E_3, can be estimated as follows:

$E[C_f] = K_f \cdot E[P_f]$; where K_f = Cost of failure and $E[P_f]$ = Expected probability of failure to detect a growing crack before reaching the critical size.

Expected probability of failure to detect a growing crack before fracture, $E[P_f]$, can be estimated as follows:

$$E[P_f] = E[P(E_3)|\, t_1<t_{cr}].P(t_1 \le t_{cr}) + E[P(E_3)|\, t_1>t_{cr}].P(t_1>t_{cr}) \tag{5.15}$$

$$= \frac{\sum_{j=1}^{N_1}\left[\prod_{i=1}^{n_j}(1-POD_i).H_i\right]}{N_1}.\left(\frac{N_1}{N}\right) + (1).\left(\frac{N_2}{N}\right) \tag{5.16}$$

$$\Rightarrow \quad E[P_f] = \frac{\sum_{j=1}^{N_1}\left[\prod_{i=1}^{n_j}[(1-POD_i).H_i]\right] + N_2}{N} \tag{5.17}$$

POD_i is probability of detection function obtained from equation 5.1 = $POD(a_i)$ where a_i is the crack size at time of ith inspection (i.e, $a_i = a(t_i)$ and $t_i = i \cdot t_{int}$).

The expected cost of repairs, $E[C_R]$, can be estimated as follows:

$$E[C_R] = E[C_{FR}] + E[C_{JR}] \tag{5.18}$$

Where $E[C_{FR}]$ = Expected cost of false repairs corresponding to event E_2

and $E(C_{JR})$ = Expected cost of justifiable repairs corresponding to event E_4.

$E[C_{FR}]$ can be estimated as follows:

$$E[C_{FR}] = E[C_{FR}|t_1 \le t_{cr}].P(t_1 \le t_{cr}) + E[C_{FR}|t_1 > t_{cr}].P(t_1 > t_{cr}) \tag{5.19}$$

$$E[C_{FR}] = \frac{\sum_{j=1}^{N_1}\sum_{i=1}^{n_j}[P(FR).K_R.]}{N_1}.\left(\frac{N_1}{N}\right) + \frac{\sum_{j=1}^{N_2}[(0).K_R]}{N_2}.\left(\frac{N_2}{N}\right) \tag{5.20}$$

$$\Rightarrow E[C_{FR}] = K_R.F.\left(\frac{\sum_{j=1}^{N_1}\sum_{i=1}^{n_j}[PFC.(1-H_i)]}{N}\right) \tag{5.21}$$

H_i is probability of presence a crack at inspection number i.

$E[C_{JR}]$ can be estimated as follows:

$$E[C_{JR}] = E[C_{JR}|t_1 \le t_{cr}].P(t_1 \le t_{cr}) + E[C_{JR}|t_1 > t_{cr}].P(t_1 > t_{cr}) \tag{5.22}$$

$$E[C_{JR}] = \frac{\sum_{j=1}^{N_1}\sum_{i=1}^{n_j}[P(JR).K_R]}{N_1}.\left(\frac{N_1}{N}\right) + \frac{\sum_{j=1}^{N_2}[(0).K_R]}{N_2}.\left(\frac{N_2}{N}\right) \tag{5.23}$$

$$\Rightarrow E[C_{JR}] = K_R.\left(\frac{\sum_{j=1}^{N_1}\sum_{i=1}^{n_j}[POD_i.H_i.(1-A_i)]}{N}\right) \tag{5.24}$$

Substitution in Eq. 5.9, leads to the objective function, OF, as follows:

$$OF = K_I.\left(\frac{\left[\frac{\sum_{j=1}^{N} t_{r_j,j}}{N}\right]}{t_{int}}\right) + K_R.\left(F.\frac{\sum_{j=1}^{N_1}\sum_{i=1}^{n}[PFC_i(1-H_i)]}{N} + \frac{\sum_{j=1}^{N_1}\sum_{i=1}^{n}[POD_i.H_i.(1-A_i)]}{N}\right) + K_F.\left(\frac{\sum_{j=1}^{N_1}\left(\prod_{i=1}^{n}[(1-POD_i).H_i]\right) + N_2}{N}\right) \tag{5.25}$$

Chapter 6

Application of the Model

6.1 Application 1: (Welding Joints of Ship Structures)

A welding detail located in a side shell longitudinal-transverse frame connection of ship structure is considered in this application. This detail was presented by Cramer et al. (1995) for the purpose of estimating the accumulated fatigue damage. The distribution of the stress range (mainly results in the waves) is modeled by Weibull distribution with shape parameter = 0.94 and scale parameter = 24.2 N/mm^2 as was estimated by Cramer et

al. (1995). The same detail with the same stress distribution is considered here but for the purpose of establishing the optimum inspection plan.

The initial flaw size, a_o, is modeled as a lognormally distributed random variable with a mean value of 0.5 mm and a coefficient of variation (COV) of 0.5. The critical crack size, a_{cr}, is considered to be constant at 50 mm for this application. The fatigue crack growth parameter, C, is modeled as a lognormal variable with a mean value of 2.18×10^{-13} assuming units of millimeters for crack size and $MPa.m^{1/2}$ for Δk and a COV of 0.63 . The fatigue crack growth exponent, m, is modeled as a normally distributed random variable with a mean value of 3 and COV of 0.047. The considered welding detail is not in contact with the sea water, hence the value of C and m are taken to be consistent with their value in air not in marine environment.

The repair policy dedicates the repair for any detected crack size (i.e. $a_r = 0$). Average number of stress cycles is 500,000 cycle/year (the considered detail encounters 500,000 waves in average per year and number of stress cycles is one cycle per one wave). The geometry function F(a) is taken unity for simplicity in this application. In this case equations (4.4) and (4.5) can be applied for calculating the critical number of cycles and therefore the critical time to failure "t_{cr}".

Three NDI techniques are considered in this application, Ultrasonic inspection (UI), Magnetic Particle Inspection (MI) and Liquid Penetrant Inspection (PI). The POD functions for the three NDI techniques based on data obtained from test results of a flat plate collected by Berens and Hovey (1981) are shown in Fig 6.1 and Table 6.1.

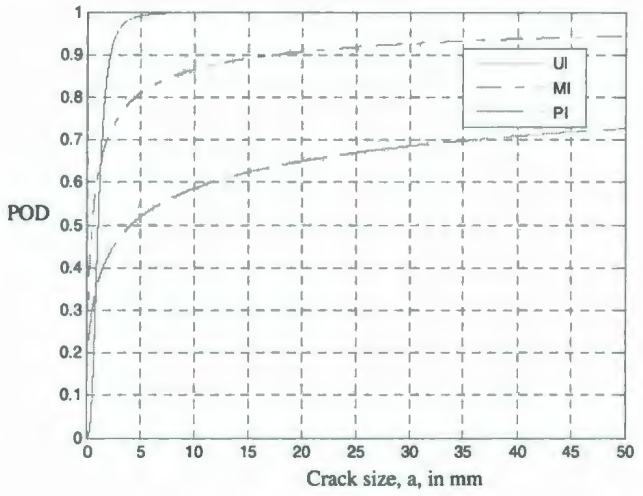

Fig 6.1: POD curves for Penetrant, PI, Magnetic, MI, and Ultrasonic, UI, inspections.

Table 6.1: Probability of detection obtained by Berens and Hovey (1981).

$POD(a) = \frac{\exp(\alpha + \beta.\ln a)}{1+\exp(\alpha + \beta.\ln a)}$		
NDI technique	α	β
UI	-0.119	2.986
MI	0.466	0.604
PI	-0.561	0.393

The relative cost of inspection (K_I) for each inspection technique, cost of repair, K_R, and cost of failure, K_F is taken as:

$K_{I,PI} : K_{I,MI} : K_{I,UI} : K_R : K_F = 1 : 1.2 : 1.5 : 2 : 20000$ \$

PFC for each inspection technique is taken as the average of the results obtained from a study was done for POD and PFC assessment of NDI techniques by Faher, et al. (1995) as follows:

$PFC_{UI} = 1.4\%$, $PFC_{MI} = 5\%$ and $PFC_{PI} = 1\%$

The applied stress intensity factor, Δk, is conservatively assumed to be greater than the threshold stress intensity range, Δk_{th}, in all the stress cycles.

By applying the proposed model (Fig. 5.1), the obtained results are shown in Table 6.2, Table 6.3 and Table 6.4.

Table 6.2: Results obtained for UI technique ($K_{I,PI}$:$K_{I,MI}$:$K_{I,UI}$:K_R:K_F = 1:1.2:1.5:2:20000 $)

	Inspection interval (year)									
	0.5	1	1.5	2	2.5	3	3.5	4	4.5	5
OF	937.97	470.80	325.03	264.59	246.21	256.40	284.49	317.23	370.91	437.42
$E[P_f]$	0	0.0002	0.0007	0.0016	0.0030	0.0051	0.0076	0.0101	0.0134	0.0173

Table 6.3: Results obtained for MI technique ($K_{I,PI}$:$K_{I,MI}$:$K_{I,UI}$:K_R:K_F = 1:1.2:1.5:2:20000 $)

	Inspection interval (year)									
	0.5	1	1.5	2	2.5	3	3.5	4	4.5	5
OF	893.30	454.07	324.07	285.26	289.53	319.80	369.34	441.15	515.57	616.62
$E[P_f]$	0.0001	0.0005	0.0014	0.0032	0.0056	0.0087	0.0122	0.0166	0.0209	0.0265

Table 6.4: Results obtained for PI technique ($K_{I,PI}$:$K_{I,MI}$:$K_{I,UI}$:K_R:K_F = 1:1.2:1.5:2:20000 $)

	Inspection interval (year)									
	0.5	1	1.5	2	2.5	3	3.5	4	4.5	5
OF	604.7	341.9	312.6	362.9	446.1	569.2	706.2	851.8	1013.2	1180.8
$E[P_f]$	0.0003	0.0022	0.0057	0.0107	0.0164	0.0236	0.0311	0.0389	0.0474	0.0561

The obtained results are shown in the following figures:

Fig. 6.2 shows the cost of inspection and cost of repair (false repairs and justifiable repairs) versus different inspection intervals for the three inspection techniques.

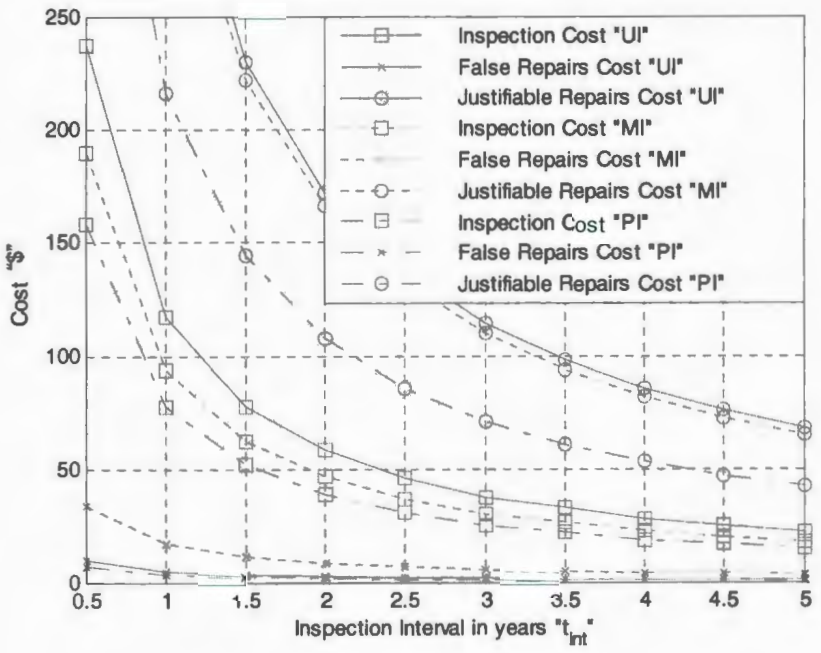

Fig. 6.2: Cost versus different inspection intervals

Figs. 6.3 and 6.4 show the expected probability of failure to detect a growing crack before reaching the critical size, $E[P_f]$, and the expected cost of failure, $E[C_f]$, versus different inspection intervals.

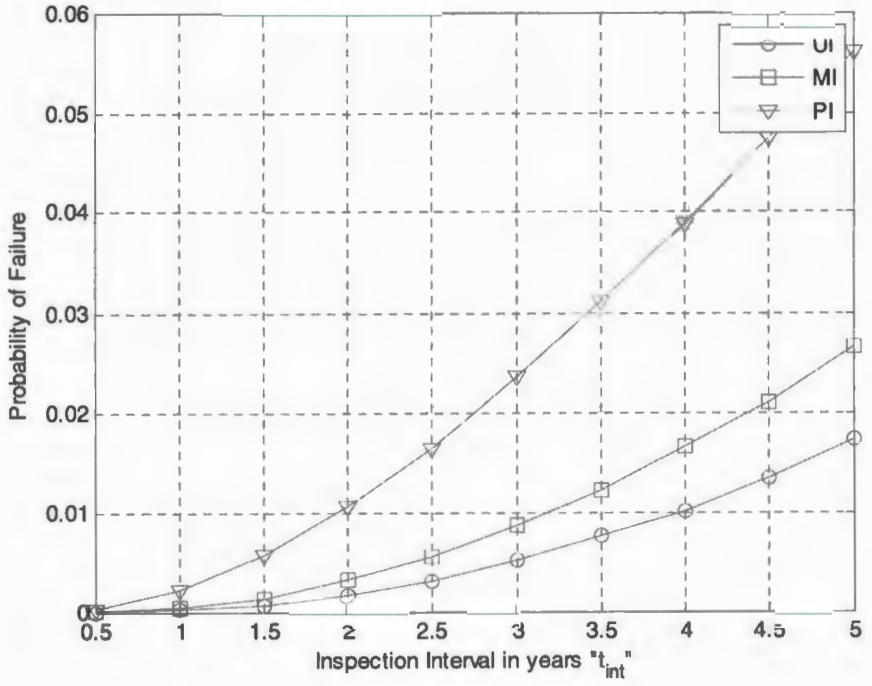

Fig. 6.3: Probability of failure to detect a growing crack before reaching the critical size versus different inspection intervals

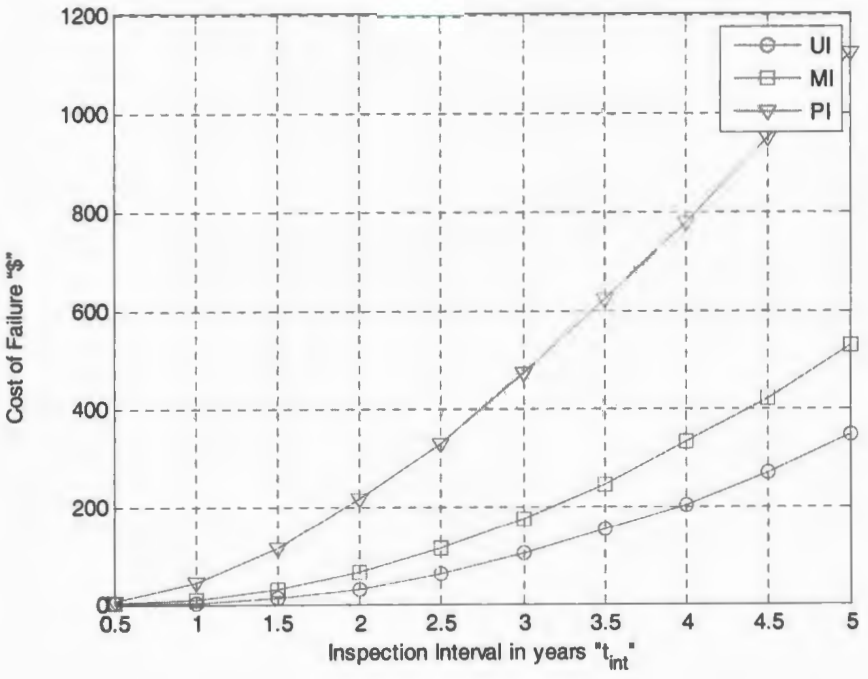

Fig. 6.4: Cost of failure to detect a growing crack before reaching the critical size versus different inspection intervals

Fig. 6.5 shows the objective function versus different inspection intervals.

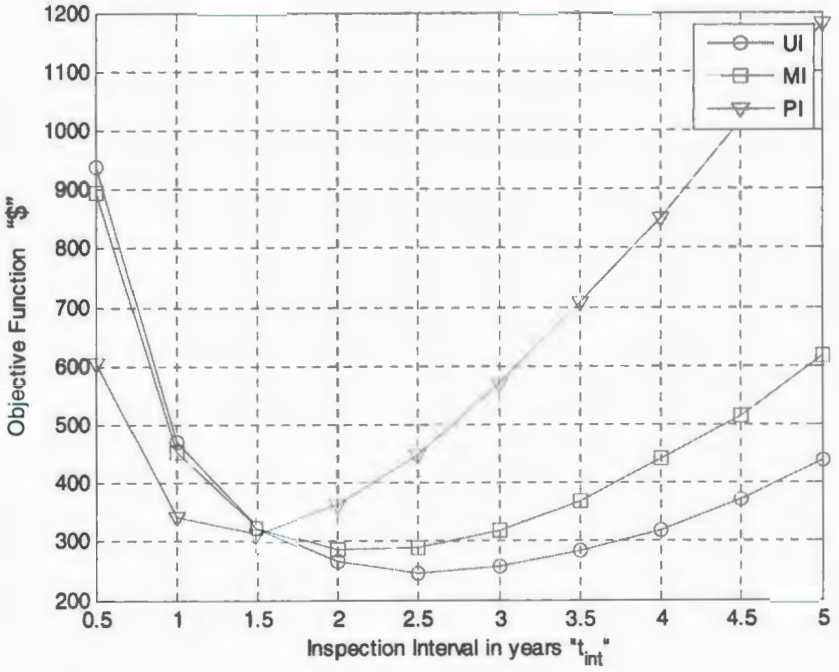

Fig. 6.5: Objective function versus different inspection intervals

Mean of the critical time to failure, $t_{cr,mean}$, obtained from all the simulations of the crack size as a function of time is obtained as 79.3 years.

From Fig. 6.5, the minimum value of the objective function and the associated inspection interval can be obtained for the three inspection technique as it is indicated in Table 6.5.

Table 6.5: Summary of the results

Inspection technique	$K_{I,PI} : K_{I,MI} : K_{I,UI} : K_R : K_F = 1 : 1.2 : 1.5 : 2 : 20000$ \$		
	Minimum value of the objective function	Optimum inspection interval in service years $t_{int,opt}$	Expected number of inspections during the lifetime $E[n] = t_{cr,mean}/ t_{int,opt}$
UI	246.2	2.5	31.72
MI	285.3	2	39.65
PI	312.6	1.5	52.87

From Table 6.5, *the optimum selection of NDI technique for this application is ultrasonic inspection "UI" with inspection interval 2.5 years.* It should be noted that probability of failure for UI at inspection interval, 2.5 years, is less than the maximum acceptable limit ($P_{f,accept} = 0.005$), Fig. 6.5.

6.2 Application 2 (Welding Joints of Subsea Pipelines)

A welding joint located in 22″ OD (thickness = 12.9 mm) sub-sea gas pipeline is considered in this application. Sub-sea pipelines are laid out on the seabed. As a result of the irregular contour of seabed surfaces, there are some parts of sub-sea pipelines are suspended and not supported by seabed soil. These suspended parts are called free spans (Fig. 6.6). Pipe in free span length is subjected to static stresses and dynamic stresses. The

static stresses are due to pipeline weight in the free span, operating temperature and pressure. The dynamic stresses are due to environmental loading caused by wave loads and/or vortex induced vibrations. The vortex induced vibrations (VIV) are caused as a result of the unstable vortices formed at the opposite side of the underwater currents direction (Fig. 6.7). The free span of the considered pipe line is 40 meters and beyond 500 meters distance from the platform.

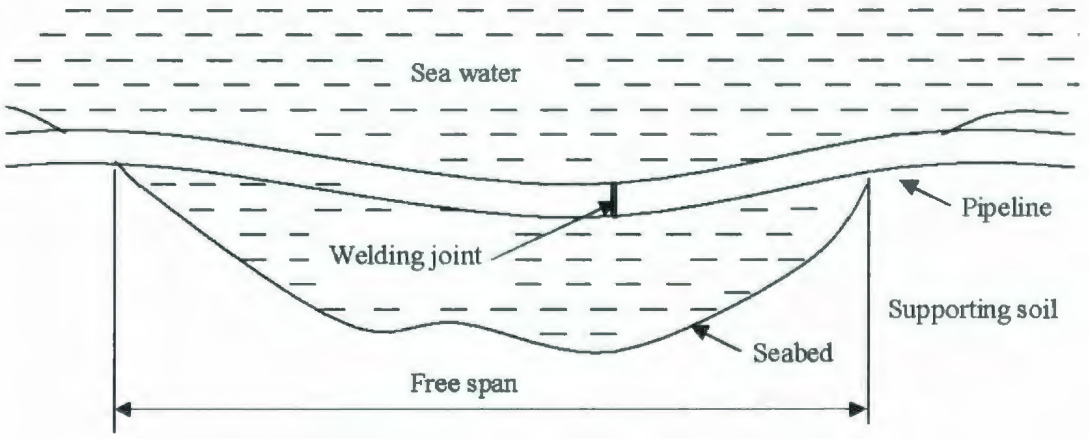

Fig. 6.6: Free span of sub-sea pipeline

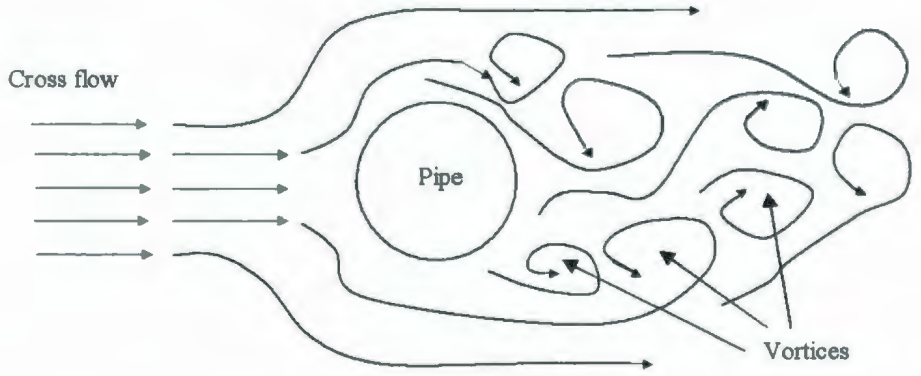

Fig. 6.7: Vortex induced vibrations of a pipe under a cross flow

The fatigue in the free span is caused by the variations in the stresses due to environmental loading. Two empirical models can be used for analysis of the case of in-line fatigue caused by direct waves induced loads or by vortex induced vibrations. The response model is relevant for current dominant conditions while the force model based on Morison's equation is applicable in wave dominant conditions. The effect of waves is significant even through the water depth is 70-80 meters [Tronsker et al. (2002)].

The distribution of the stress range ($\Delta\sigma$) in the free span of subsea pipelines due to vortex induced vibrations can be modeled by Weibull distribution [Tronsker et al. (2002)] assuming that the welding joint is located at the middle of the free-span at 3 and 9 o'clock position (i.e at position of the maximum applied stresses). The welding joint is the critical point in the pipeline due to welding flaws and stress concentration so it should be inspected at regular intervals to ensure the safety of the pipe line for which we are seeking for the optimum selection of the NDI technique and its associated optimum inspection interval.

The cumulative probability density function of Weibull distribution for the stress range ($\Delta\sigma$) is:

$$F(\Delta\sigma) = 1 - \exp\left[-\left(\frac{\Delta\sigma}{\theta}\right)^{\beta}\right] \tag{6.1}$$

The two parameters (θ and β) of the stress range ($\Delta\sigma$) Weibull distribution due to VIV are dependent on the diameter of the pipe line and free span length as follows [Tronsker et al. (2002)].

22″ OD:

Span length	θ	β	# Stress cycles/year
40 m	4.9 MPa	0.8	$3.6x10^5$
45 m	11.5 MPa	1.2	$2x10^6$
50 m	13.4 MPa	1.5	$2.4x10^6$

14″ OD:

Span length	θ	β	# Stress cycles/year
22.5 m	1.15 MPa	0.84	$0.59x10^1$
25 m	2.24 MPa	0.74	$1.2x10^4$
27.5 m	2.98 MPa	0.76	$4.5x10^5$
30 m	5.68 MPa	0.98	$2.3\ x10^6$

Tronsker et al. (2002) found that, for the considered 22″ pipeline, free-span survey should be performed with intervals not exceeding 3 years to ensure a failure probability, due to reaching the span length to the critical length, not exceeding 10^{-4} and should be performed annually to ensure a failure probability not exceeding 10^{-5}.

In the optimization problem for selecting the optimum NDI technique, it is assumed that the free span will be surveyed at regular intervals in order to keep it not exceeding the critical length (50 meters), so the stress range distribution is not changed and can be

conservatively modeled by Weibull distribution at the critical length (50 meters) with θ = 13.4 Mpa and β = 1.5. The average number of stress cycles is 2.4×10^6 cycle/year.

The initial (pre-service) flaws size (depth), a_o, is modeled as a lognormally distributed random variable with a mean value of 0.97 mm and a standard deviation of 0.504 mm [Tronsker et al. (2002)].The critical crack size (depth of the crack at which leakage will occur), a_{cr} is considered to be constant at 5 mm for this application. The fatigue crack growth parameter, C, is modeled as a lognormal variable with a mean value of 6.06×10^{-13} assuming units of millimeters for crack size and $MPa.mm^{1/2}$ for fracture toughness and a standard deviation of 1.58×10^{-13} mm [Tronsker et al. (2002)]. The value of the material parameter, C, is higher in this application than its value in the previous application (ship structure welding joint) because of the environmental effect under sea water which accelerate the cracks propagation (corrosion fatigue) while in ship application, the considered welding joint is not in contact with the sea water (i.e only fatigue). The fatigue crack growth exponent, m, is modeled as a normally distributed random variable with a mean value of 3 and a standard deviation of 0.14 mm. The repair policy dedicates the repair for any detected crack size (i.e. $a_r = 0$). The geometry function F(a) is taken also unity for simplicity in this application.

Maximum acceptable probability of failure to detect a growing crack before reaching the critical size is taken as 0.001 for this application.

Two NDI techniques are considered in this application, Ultrasonic inspection (UI) and Magnetic Inspection (MI) while Liquid Penetrant Inspection (PI) is not applicable under water. POD functions for UI and MI are assumed to be the same as presented in ship

structure application. The relative costs of inspection (K_I), cost of repair, K_R, and cost of failure, K_F, are taken as:

$K_{I,MI} : K_{I,UI} : K_R : K_F = 1.2 : 1.5 : 10 : 20000$

For the lack of data of PFC of the two NDI techniques when used for inspecting sub-sea pipelines while the noise in subsea environmental could be different from the noise in air, PFC for each inspection technique is also assumed to be the same as presented in ship structure application ($PFC_{UI} = 1.4\%$ and $PFC_{MI} = 5\%$).

The applied stress intensity factor, Δk, is conservatively assumed to be greater than the threshold stress intensity range, Δk_{th}, in all the stress cycles. In this case, the sequence of the applied variable stress does not affect the accumulated crack growth and the crack growth can be obtained by effective stress method.

By applying the proposed model (Fig. 5.1), the obtained results are shown in Table 6.6, Table 6.7 and the following figures.

Table 6.6: Results obtained for UI technique ($K_{I,MI}$:$K_{I,UI}$:K_R:K_F = 1.2:1.5:10:20000 $)

	Inspection interval (year)									
	0.5	1	1.5	2	2.5	3	3.5	4	4.5	5
OF	525.63	268.96	188.30	157.87	155.35	168.31	197.58	248.23	301.77	377.84
$E[P_f]$	0.0003	0.0005	0.0009	0.0015	0.0027	0.0042	0.0063	0.0093	0.0124	0.0164

Table 6.7: Results obtained for MI technique ($K_{I,MI}$:$K_{I,UI}$:K_R:K_F = 1.2:1.5:10:20000 $)

	Inspection interval (year)									
	0.5	1	1.5	2	2.5	3	3.5	4	4.5	5
OF	458.92	241.55	186.32	184.63	216.64	271.84	346.80	447.95	553.31	682.94
$E[P_f]$	0.0003	0.0008	0.0019	0.0037	0.0064	0.0100	0.0142	0.0197	0.0253	0.0320

Fig. 6.8 shows the cost of inspection and cost of repair (false repairs and justifiable repairs) versus different inspection intervals for the two inspection techniques.

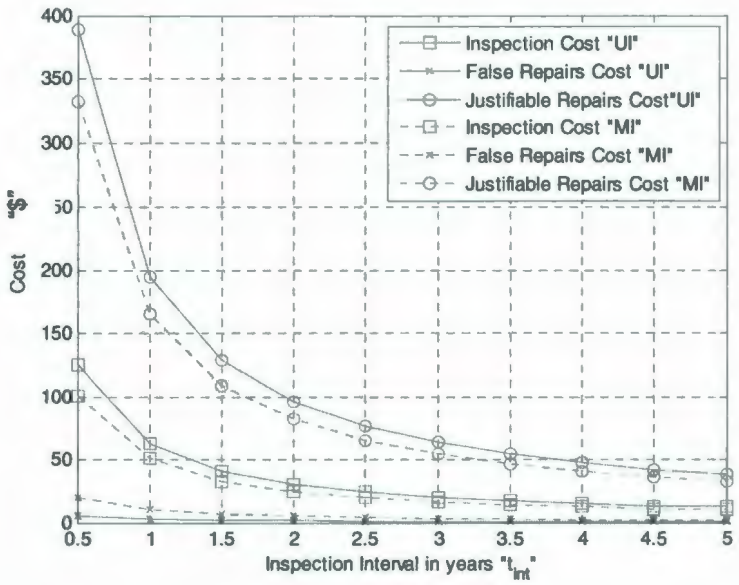

Fig. 6.8: Cost versus different inspection intervals (subsea pipelines)

Figs. 6.9 and 6.10 show the expected probability of failure, $E[P_f]$, and cost of failure, $E[C_f]$, to detect a growing crack before reaching the critical size versus different inspection intervals.

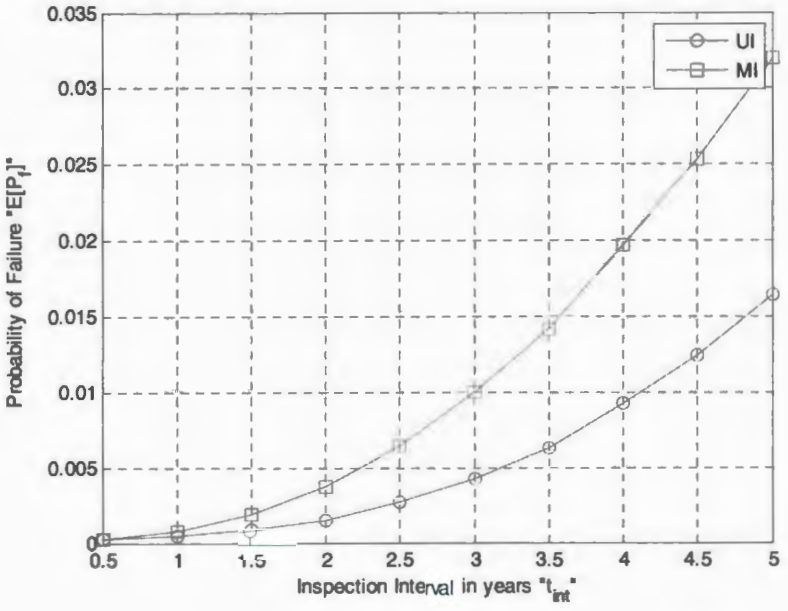

Fig. 6.9: Probability of failure to detect a growing crack before reaching the critical size versus different inspection intervals (subsea pipelines)

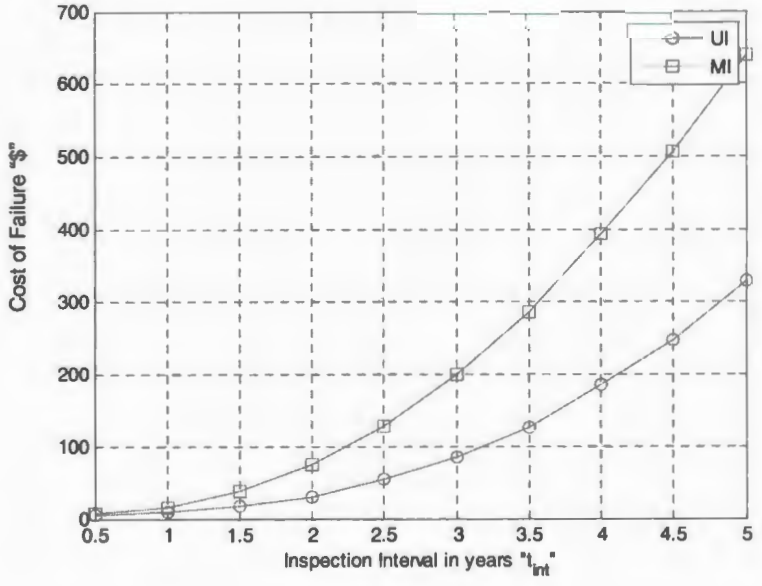

Fig. 6.10: Cost of failure to detect a growing crack before reaching the critical size versus different inspection intervals (subsea pipelines)

Fig. 6.11 shows the objective function versus different inspection intervals.

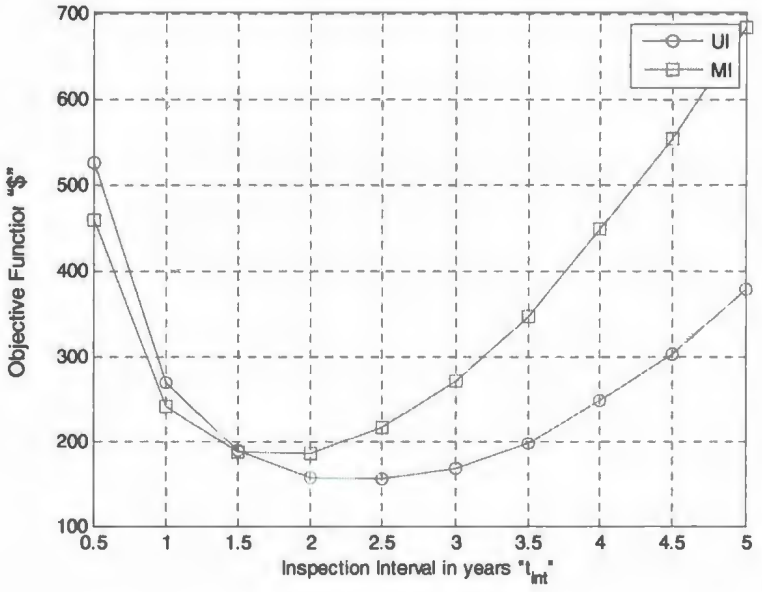

Fig. 6.11: Objective function versus different inspection intervals (subsea pipelines)

Mean of the critical time to failure, $t_{cr,mean}$, obtained from the simulation of the crack growth rate, is 42.5 year with standard deviation of 35.2 year.

From Fig. 6.9, Table 6.6 and Table 6.7, the maximum acceptable inspection interval which keeps probability of failure, $E[P_f]$, not exceeding 0.001 (safety constraint) is 1.5 year for UI and 1 year for MI. From Fig. 6.11, the minimum value of the objective function is 155.35 (located at inspection interval 2.5 years) for UI and 184.6307 (located at inspection interval 2 years) for MI. By comparing the minimum value of the objective function of the two inspection techniques, it is preferable to use UI technique with inspection interval 1.5 year, but for the safety constraint, the inspection interval should not exceed 1.5 year for UI and 1 year for MI. By comparing the value of the objective function at inspection interval of 1.5 years for UI which is 188.30 and at 1 years for MI

which is 241.55, leads to *the optimum selection between the two techniques (UI and MI) is UI with inspection interval of 1.5 years* where that selection shall ensure the minimum possible value of the objective function taking into consideration the safety constraint ($E[P_f] < 0.001$).

Chapter 7

Discussion and Conclusions

7.1 Discussion

1- Cost of inspection and cost of repairs increase as the inspection interval decreases (Figs. 6.2 and 6.8) because the shorter the inspection interval is the greater the expected number of inspections during the lifetime will be. This leads to high cost of inspection and high cost of repairs.

2- The longer the inspection interval is the higher the probability of failure. This will cause a higher cost of failure (Figs. 6.3, 6.4, 6.9 and 6.10). This is caused by the fact that the longer the inspection interval is the smaller the expected number of inspections during the lifetime will be.

3- Probability of failure when using the ultrasonic (UI) technique is lower than when using the magnetic particle (MI) technique or the penetrant (PI) technique (Figs. 6.3 and 6.9) because the POD for the ultrasonic technique is higher than the POD for both the magnetic particle technique and the penetrant technique.

4- The inspection interval which is required to achieve the optimum cost in case of the ultrasonic technique is larger than in the case of the magnetic particle technique or the penetrant technique because the ultrasonic technique has better detectability (POD), (Figs 6.5 and 6.11).

5- The objective function for all cases considered is valley-shaped.

6- After applying the safety constraint, a maximum acceptable inspection interval can be obtained at which the probability of failure equals the maximum acceptable probability of failure ($P_{f,accept}$). The probability of failure is taken as 0.005 for the ship structure application and 0.001 for the subsea pipelines. The optimal inspection interval for an NDI technique can be found at the minimum value of the objective function curve taking into consideration the optimum inspection interval should be less than the maximum acceptable inspection interval for the safety constraint. If the maximum acceptable inspection interval is less than the inspection interval at the minimum value of the objective function, the optimum inspection interval should be the same as the maximum acceptable inspection interval.

7- The cost of failure depends on the criticality of the inspected detail and the cost of each repair depends on the repair method, the location of that repair and shutdown

cost (if required). The change in the objective function as a result of the change in the failure cost is studied for different relative cost of failure, k_F, keeping the cost of each repair, k_R, (the repair policy is $a_r = 0$) and the cost of inspection, k_I, constant. The valley shaped curve of the objective function is shifted up and to the left when increasing the relative cost of failure, k_F, which makes the optimum inspection interval shorter (Figs. 7.1 and 7.2). The change in the objective function as a result of the change in repair cost, k_R, is studied for different relative cost of repair, k_R, (the repair policy is $a_r = 0$) keeping cost of failure, k_F, and cost of each inspection, k_I, constant. The valley shaped curve of the objective function is shifted up and to the right when increasing the relative cost of repair, k_R, which makes the optimum inspection interval longer (Figs. 7.1 and 7.2). The ultrasonic inspection technique, UI, is the optimal technique for the two cases studied in this thesis, see Figs. 7.1 to 7.4.

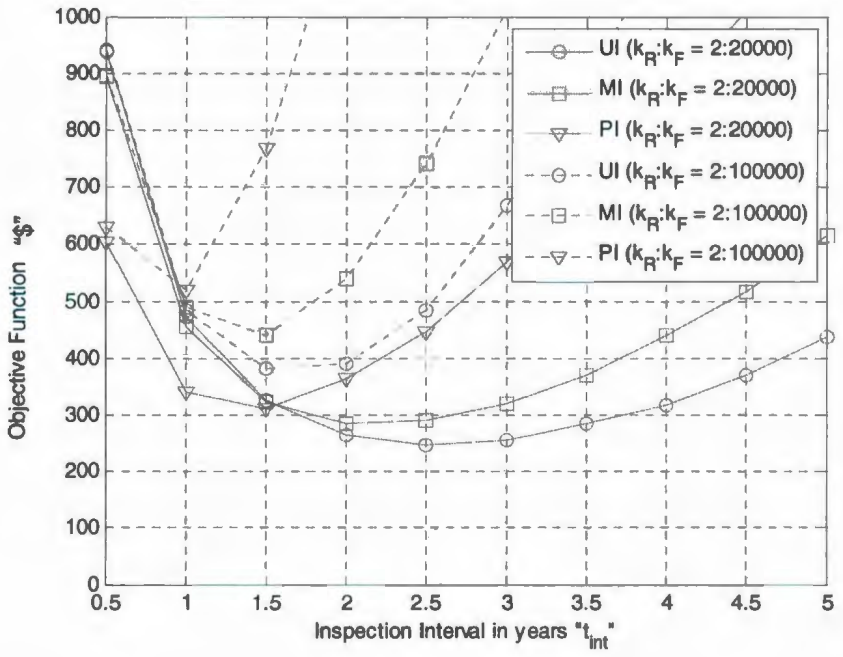

Fig. 7.1: Objective function for different relative cost of failure, k_F (ship structure)

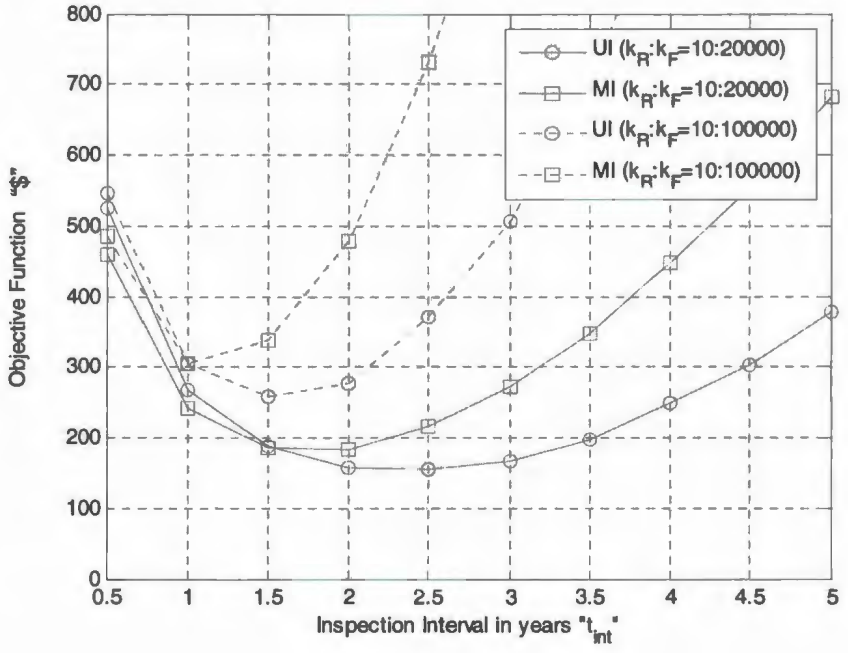

Fig. 7.2: Objective function for different relative cost of failure, k_F (subsea pipelines)

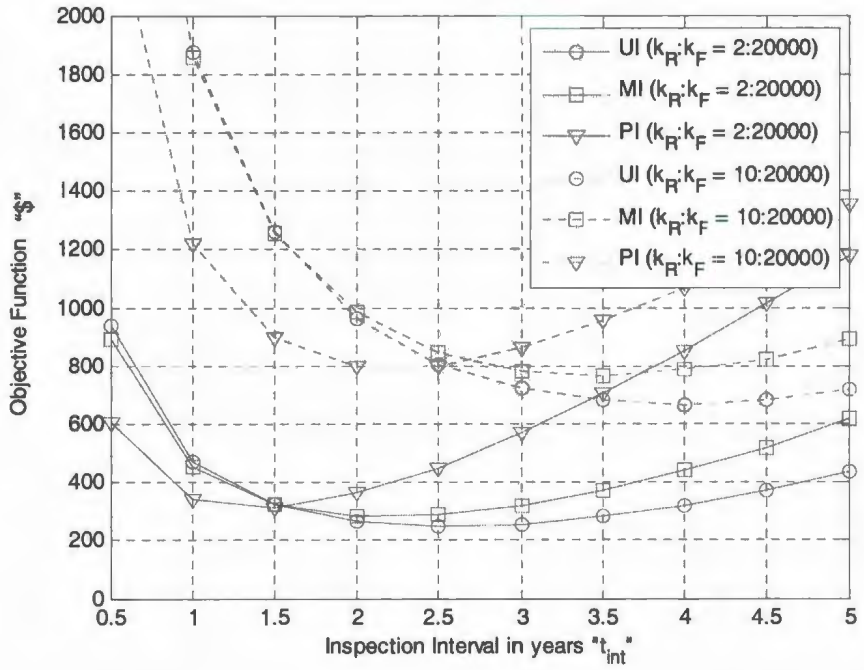

Fig. 7.3: Objective function for different relative cost of repair, k_R (ship structure)

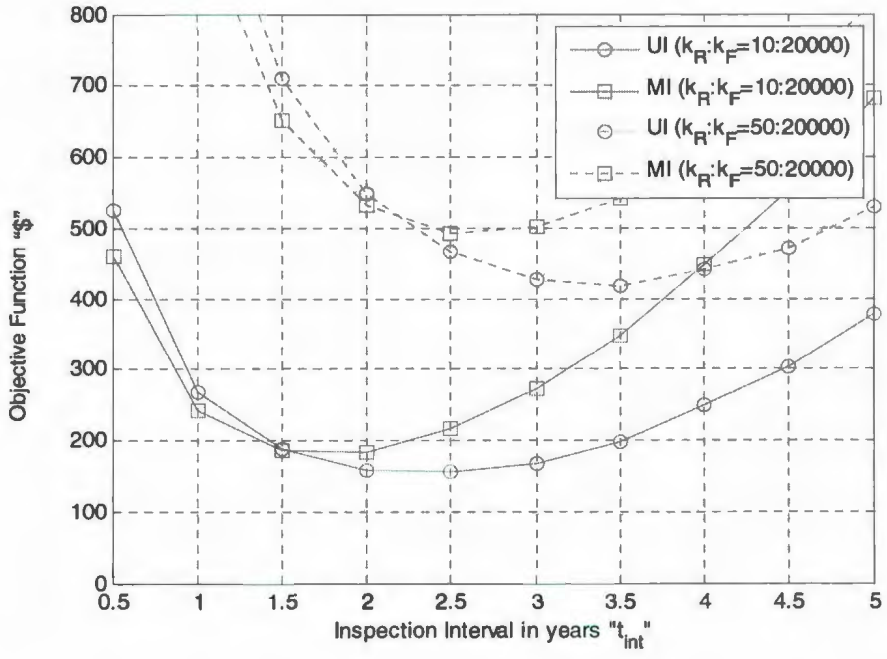

Fig. 7.4: Objective function for different relative cost of repair, k_R (subsea pipelines)

7.2 Conclusions

A probabilistic optimization model for selecting an optimal NDI technique and an associated inspection interval has been presented. The objective function including inspections cost, repairs cost over the lifetime and cost of failure is formulated as a function of the reliability of the NDI technique (Probability of Detection function "POD" and the Probability of False Calls "PFC"), the condition of the inspected component (critical time to failure "t_{cr}", the probability of the presence a crack in the inspected asset "H"), and the inspection interval "t_{int}". The decision variables (controllable) are POD, PFC and t_{int}. The objective function is minimized subject to the safety constraint that the probability of failure to detect a growing crack before reaching the critical size, $E[P_f]$, does not exceed a predefined level, $P_{f,accept}$.

The probability of each inspection outcome is estimated using an event tree of the possible inspection outcomes. Cracks are growing with time so probability of presence of a crack, H, is calculated based on the distribution of the crack size at inspection time. The optimization problem is solved for different inspection techniques. The optimum nondestructive inspection technique and its associated inspection interval are obtained by comparing the values of the objective functions for the inspection techniques taking into consideration the safety constraint.

The model was applied to two case studies: a part of the structure of a ship and a segment of a subsea pipeline. In both cases, it was found that the ultrasonic technique is optimal.

References

Apeland, S., Aven, T. (1999). Risk Based Maintenance Optimization: Fundamental Issues. *Reliability Engineering and System Safety, 67, 285-292.*

API 581, First Edition, May 2000. Risk Based Inspection Resource Document.

ASME (1999). Risk Based Inspection (RBI). A Risk Based Approach to Planned Plant Inspection. *Health and Safety Executive – Hazardous Installation Division,* CC/TECH/SAFETY/8.

ASME Boiler and Pressure Vessel Code, section XI, 2004 Edition. Rules For Inservice Inspection of Nuclear Power Plant Components. The American Society of Mechanical Engineers, New York, New York.

Balkey, Art, Bosnk (19998). ASME Risk Based In service Inspection and Testing: An Outllook to the future. Society for risk analysis, 18(4).

Berens, A.P. and Hovey, P.W. (1981). Evaluation of NDE Reliability Characterization. AFWAL-TR-81-4160, 1, Air Force Wright-Aeronautical Laboratory, Wright-Patterson Air Force Base, Dayton, Ohio.

Charles, J. H. (2003). Handbook of Nondestructive Evaluation. McGraw-Hill Books, Two Penn Plaza, New York, NY 10121-2298. ISBN 0-07-028121-7.

Chung, Hsin-Yang, Manuel, L. and Frank, K.H. (2003). Reliability-Based Optimal Inspection for Fracture-Critical Steel Bridge Members. *Transportation Research Record*, 1845, 39-47

Chung, Hsin-Yang, Manuel, L. and Frank, K.H. (2006). Optimal Inspection Scheduling of Steel Bridges Using Non Destructive Testing Techniques. Journal *of Bridge Engineering*. 11, 3, 305-319.

Cramer, E.H., and Friis-Hansen, P., (1992). Reliability Based Optimization of Multi-Component Welded Structures. OMAE, II, Safety and Reliability ASME 1992, Proceeding Of The 11th International Conference on Offshore Mechanics And Arctic Engineering, Calgary, Canada. 2, 265-271.

Cramer, E.H., Loseth R., and Olaisen K. (1995). Fatigue Assessment of Ship Structures. *Marine Structures*. 8, 359-383.

Deardorff, F. (2002). Section XI Flaw Acceptance Criteria and Evaluation Using Code Procedures. Companion Guide to the ASME Boiler and Pressure Vessels Code. 2, 395-421.

Dey, P.M. (2001). A Risk-Based Model for Inspection and Maintenance of Cross-Country Petroleum Pipelines. *Journal of Quality in Maintenance Engineering*. 40, 24-31.

Faher, A., Forsyth, D., Bullock, M., Wallace, W., Ankara, A., Kompotiaties L. and Goncalo, H.F.N. (1995). POD Assessment of NDI Procedures Using Round Robin Test. Advisory Group for Aerospace Research & Development (AGARD), Report 809, ISBN 92-836-1010-5.

Fang, Bingyan; Han, Enhou; Zhu, Ziyong; Wang, Jianqiu; Ke, Wei Source (2002). Stress corrosion cracking of pipeline steels. *Journal of Materials Science and Technology*, 18, 1, 3-6

Fujiyama, Nagai, Akikuni, Fujiwara, Furuya, Mastsumoto, Takagi, Kawabata (2004). Risk-Based Inspection and Maintenance Systems for Steam Turbines. *International Journal of Pressure Vesseles and Piping.* 81(10-11), 825-835.

Gooch, T. G. (1986). Review of Stress Corrosion Cracking of Welded Duplex Ferritic/Austenitic Stainless Steels. *Welding in the World, Le Soudage Dans Le Monde.* 24, 7-8, 148-167.

Hagemeijer, Kerkveld (1995). Methodology for risk based inspection of pressurized systems. *Proceedings of the Institution of Mechanical Engineers,* Part E. *Journal of Process Mechanical Engineering.*

Harris, DO., (1992). Probabilistic Fracture Mechanics with Applications to Inspection Planning and Design. *AD (American Society of Mechanical Engineers).* 28, 57-76.

Heasler, P.G., Taylor T.T., and Doctor, S.R. (1993). Statistically Based Reevalution of PICS-II Round Robin Test Data. NUREG/CR-5410, US Nuclear Regulatory Commission, Washington, DC.

Kallen, M.J. (2002). Risk Based Inspection in the Process and Refining Industry. Master Thesis, Faculty of Information Technology and Science, Technical University of Delft, The Netherlands.

Kallen, M.J., Noortwijk, J.M. Van (2004). Optimal Inspection and Replacement Decisions for Multiple Failure Modes. *Probabilistic Safety Assessment and Management* (PSAM7) ESREL'04). *Proceedings of the 7th International Conference on Probabilistic Safety Assessment and Management, Berlin, Germany.*

Kallen, M.J., Noortwijk, J.M. Van (2005). Optimal maintenance Decisions Under Imperfect Inspection. *Reliability Engineering and System Safety*. 90(2-3), 177-185.

Khan, F.I., Haddara, M. (2003). Risk-Based Maintenance (RBM): A Quantitative Approach for Maintenance/Inspection Scheduling and Planning. *Journal of Loss Prevention in the Process Industrie*. 16,561-573.

Khan, F.I., Haddara, M. (2004a). Risk-Based Maintenance (RBM): A new Approach for Process Plant Inspection and Maintenance. *Process Safety Progress*. 23, 4, 252-265.

Khan, F.I., Haddara, M (2004b). Risk Based Maintenance of ethylene Oxide Production Facilies. *Journal of Hazardous Materials*. A108, 147-159.

Khan, F.I., Haddara, M. ., Bhattacharya, S. (2006). Risk Based Integrity and Inspection Modeling of Process Components. *Risk Analysis*. 26.

Krishnasamy, L., Khan, F., Haddara, M. (2005). Development of Risk-Based Maintenance (RBM) Strategy for a Power-Generating Plant. *Journal of Loss Prevention in the Process Industries*. 18, 2, 69-81.

Moan T, Va` Rdal OT, Hellevig N-C, Skjoldli K., (1997). In-Service Observations of Cracks In North-Sea Jackets. A Study on Initial Crack Depth and POD Values. In:

ASME NY, Editor. Proceedings of the 16th International Conference on Offshore Mechanics and Arctic Engineering, 2.

NDT Education Resource Center (2001), Center for Nondestructive Evaluation, Ames, USA.

Nessim, M.A., Stephens, M.J. (1995). Risk Based Optimization of Pipeline Integrity Maintenance. *OMAE,* V, 303-314.

Nessim, M.A>, Stephens, M. J., Zimmerman, T.J.E. (2000). Risk Based Maintenance Planning for Offshore Pipelines. *Proceedings of the Annual Offshore Technology Conference*. 2, 791-800.

Noori, S.A., Price, J. (2005). Case Study of the use of API 581 on HK and HPMaterial Furnace Tubes. *Journal of Pressure Vessel Technology*. 127, 49-54.

Paris, P.C. and Erdogan, F., (1963). Critical Analysis of Crack Propagation Laws. *Basic Eng.*, 85, 528-534.

Ragab, Abel-Rahman and Bayoumi, Salah Eldin. (1999) Engineering Solid Mechanics Fundamentals and Applications Book. Boca Raton, Fl.: CRC Press, ISBN 0849316073.

Rouhan, A. and Schoefs, F. (2003). Probabilistic Modeling of Inspection Results for Offshore Structures. *Journal of Structural Safety*. 25, 397-399.

Schilling, C.G., Klippstein, K.H., Barsom J.M., and Blake, G.T. (1978). Fatigue of Welded Steel Bridge Members Under Variable Amplitude Loadings. National

Cooperative Highway Research Program Rep. No. 188, Transportation Research Board, National Research Council, Washington, D.C.

Schueller, G.I. and Kuntiyawichai, K. (2006). Reliability Based Optimization Approach for Nondestructive Inspection Planning. *47th AIAA/ASME/ASCE/AHS/ ASC Structures, Structural Dynamics and Materials Conference*. Newport, R.I., 8, AIAA 2006-2064, 5659-5671.

Staat, M. (1993). Sensitivity of and Influences on the Reliability of an HTR-Module Primary Circuit Pressure Boundary. *12th International Conference on Structural Mechanics in Reactor Tech.* Elsevier, Amsterdam, 147-152.

Straub, Faber (2005). Risk Based Inspection Planning for Structural Systems. *Structural Safety.* 27, 4, 335-355.

Tanaka, S., Ichikawa M., and Akita, S., (1981). Variability of m and C in the Fatigue Crack Propagation Law $(da/dn) = C(\Delta K)^m$, *Fract.* 17, 121-124.

Thurlbeck SD, Stacey A, Sharp JV and Nichols NW., (1996). Welding Fabrication Defects in Two Offshore Steel Jacket Structures. In: ASME Editor. Proceeding of the 15th International Conference on Offshore Mechanics and Arctic Engineering, *Materials Engineering*, 3, 232–46.

Tronskar, J.P., Sigurdsson, G., Kiefer, J.H. and Lewis, C. (2002). Probabilistic inspection optimization of Free-Span Surveys for Subsea Gas Pipelines. 21st International Conference on Offshore Mechanics and Artic Engineering, Oslo, Norway, 4, 59-72.

Vaurio, J.K. (1995). Optimization of Test and Maintenance Intervals Based on Risk and Cost. *Reliability Engineering and System Safety.*

Vesely, Belhadj, Rezos (1994). PRA Important Measures for Maintenance Prioritization application. *Reliability Engineering and System Safety.* 43.

White (2005). Development of Crack Growth Rate Disposition Curves for Primary Water Stress Corrosion Cracking (PWSCC) of Alloy 82, 182. Proceeding of the Twelfth International Conference on Environmental Degradation of Materials in Nuclear Power Systems-Water Reactors, 511-531.

Appendix

Matlab Program for the Proposed Optimization Model

```
clear all
% No. of simulations = s
% inspection interval = tint (years)
% cost of one inspections = ki
% cost of failure = kf
% critical time to failure = tcr
% critical crack size = acr (mm)
% probability of detection of the inspection technique for one of the
candidates inspection techniques = POD
% probability of false calls of the inspection technique for one of the
candidates inspection techniques= PFC
% alpha of the POD function  = v
% beta of the POD function  = p
% initial crack size (preexisting cracks) = ao
% coeff. of variation and mean of preexisting cracks = covao and muao
% parameters of weibull distribution for the variable stress = b1 and b2
% probability of having a crack = Gamma
% time = t
% frequency of loading = f
s = input ('s = ')
%acr = 5 for pipeline application;
acr = input (' acr = ')
%v = -0.119 for UI;
v = input (' v = ')
%p = 2.986 for UI;
p = input (' p = ')
%PFC = 0.014 for UI;
PFC = input (' PFC = ')
%Ki = 1.5 for UI;
Ki = input (' Ki = ')
%Kr = 10 for pipeline application;
Kr = input (' Kr = ')
%Kf = 20000;
Kf = input (' Kf = ')
%covao = 0.52 for pipeline application;
covao = input (' covao = ')
%muao = 0.97 for pipeline application;
muao = input (' muao = ')
%b1 = 13.4 for pipeline application;
b1 = input (' b1 = ')
%b2 = 1.5 for pipeline application;
b2 = input (' b2 = ')
%f = 2400000 for pipeline application;
f = input (' f = ')
% lognormal distribution parameter estimation
sigmasqyao = log(1+covao^2);
sigmayao = sigmasqyao^0.5;
muyao=log(muao)-0.5*sigmasqyao;
```

```
covc = input (' covc = ')
muc = input (' muc = ')
% covc = 0.26 for pipeline application;
% muc =6.06e-13 for pipeline application;
sigmasqyc = log(1+covc^2);
sigmayc = sigmasqyc^0.5;
muyc=log(muc)-0.5*sigmasqyc;
for t = 1:300
    T(t) = t;
    k1=1;
    for x=1:ceil(s/5)
        disp(x)
        disp(t)
    %m = random ('normal' , 3 , 0.14);
    m = normrnd(3 , 0.14);
    %c = random('lognormal',muyc, sigmayc);
    c = lognrnd(muyc, sigmayc);
    ao = lognrnd(muyao,sigmayao);
    SRE = b1*gamma((1 + m/b2))^(1/m);
    if m ==2
        tcr=log(acr/ao)/(3.14*c*SRE^2*f);
    else
        tcr = ((acr)^((2-m)/2)-ao^((2-m)/2))/(((2-
m)/2)*3.14^(m/2)*c*SRE^m*f);
    end
    if t<tcr
        if m == 2
            a = ao*exp(3.14*c*SRE^2*f*t);
        else
        a = (ao^((2-m)/2)+((2-m)/2)*3.14^(m/2)*c*SRE^m*f*t)^(2/(2-m));
        end
    A(k1) = a;
    k1=k1+1;
    end
    end
    Mean(t) = mean(A);
    StD(t)= std(A);
end
k=0;
for tint = 0.5:0.5:5
    k=k+1;
    disp('inspection interval'), disp(tint)
    Tint(k) = tint;
sumn = 0;
sumtr = 0;
sumtcr=0;
SumPr1 = 0;
SumPr2 = 0;
AvgPfs = 0;
s1=0;
for j = 1:s
    disp (j)
    disp(tint)
    %m = random ('normal' , 3 , 0.14);
```

```
    m = normrnd(3 , 0.14);
    %c = random('lognormal',muyc, sigmayc);
    %ao = random('lognormal',muyao,sigmayao);
    c = lognrnd(muyc, sigmayc);
    ao = lognrnd(muyao,sigmayao);
    SRE = b1*gamma((1 + m/b2))^(1/m);
    if m ==2
        tcr=log(acr/ao)/(3.14*c*SRE^2*f)
    else
        tcr = ((acr)^((2-m)/2)-ao^((2-m)/2))/(((2-
m)/2)*3.14^(m/2)*c*SRE^m*f);
    end
    Tcr(j) = tcr;
    z = tcr/tint;
    n = floor(z);
    if tint>tcr
        Pnd = 1;
        P3 = 1;
        Pfs = 1;
    end
    if tint<tcr
        s1=s1+1;
        Pnd = 1;
        P3 = 1;
        Pfs = 1;
        for i = 1 : n
            t = i*tint;
            if m == 2
                a = ao*exp(3.14*c*SRE^2*f*t)
            else
                a = (ao^((2-m)/2)+((2-
m)/2)*3.14^(m/2)*c*SRE^m*f*t)^(2/(2-m));
            end
            if t <300
            Sigmaaonew = StD(ceil(t));
            Muaonew = Mean(ceil(t));
            else
                Sigmaaonew = StD(300);
                Muaonew = Mean(300);
            end
            Covaonew=Sigmaaonew/Muaonew;
            Sigmasqyaonew = log(1+Covaonew^2);
            Sigmayaonew = Sigmasqyaonew^0.5;
            Muyaonew=log(Muaonew)-0.5*Sigmasqyaonew;
            %Gamma = cdf('lognormal',a,Muyaonew,Sigmayaonew);
            Gamma = logncdf(a,Muyaonew,Sigmayaonew);
            POD = (exp(v+p*log(a)))/(1+(exp(v+p*log(a))));
            Pndnew = 1-POD;
            Pfsnew = (1-POD)*Gamma;
            Pr1 = PFC*(1-Gamma);
            Pr2 = POD*Gamma;
            SumPr1 = SumPr1 + Pr1;
            SumPr2 = SumPr2 + Pr2;
            Pfs = Pfs*Pfsnew;
```

```
        end
    end
    AvgPfs = AvgPfs + Pfs;
    sumn = sumn + n;
    sumtcr = sumtcr + tcr;
end
AvgPfs1 = AvgPfs/s;
Pfnews(k)=AvgPfs1;
navg = floor(sumn/s);
savenavg(k) = navg;
SumPr1 = SumPr1/s;
SumPr2 = SumPr2/s;
ci = navg*Ki;
Ci(k) = ci;
cfnews = AvgPfs1*Kf;
Cfnews(k) = cfnews;
cr1s = SumPr1*Kr;
cr2s = SumPr2*Kr;
Cr1s(k) = cr1s;
Cr2s(k) = cr2s;
costnews = ci + cfnews ;
COSTnews(k) = costnews;
avgtcr = sumtcr/s;
end
disp('Results for this inspection technique')
disp('Inspection Cost')
disp(Ci)
disp('False repairs Cost')
disp(Cr1s)
disp('Justifiable repairs Cost ')
disp(Cr2s)
disp('Risk')
disp(Cfnews)
disp('Probability of Failure ')
disp(Pfnews)
disp(COSTnews)
disp(Objective Function "OF"')
disp(Ci+Cfnews+Cr1s+Cr2s)
OFmin=min(COSTnews+Cr1s+Cr2s);
disp('Minimum value of the Objective function "OFmin"')
disp(OFmin)
disp('Expected lifetime "tcr,mean" =')
disp(mean(Tcr))

dfittool(Tcr)

subplot 231;
xlabel('Inspection Interval in years "t_i_n_t"')
ylabel('Objective Function "OF"')

hold on
plot(Tint,COSTnews+Cr1s+Cr2s,'-o')
grid
```

```
hold off
subplot 232;
plot(Tint,Ci,':s')
hold on
plot(Tint,Cr1s,'-x')
plot(Tint,Cr2s,'-*')
xlabel('Inspection interval in years "t_i_n_t"')
ylabel('Cost')

legend('Inspection Cost','False Repairs Cost','Justifiable Repairs
Cost')
grid

hold off
subplot 233;
plot(Tint,Cfnews,'-v')
xlabel('Inspection interval in years "t_i_n_t"')
ylabel('Risk')

grid

hold off
subplot 234;
plot(Tint,Pfnews,'-v')
xlabel('Inspection interval in years "t_i_n_t"')
ylabel('Probability of Failure "E[P_f]"')

grid

hold off
subplot 235;
plot(T,Mean)
xlabel('time "years"')
ylabel('Mean')
title('Mean of cracks size at a given time')
grid

hold off
subplot 236;
plot(T,StD)
xlabel('time "years"')
ylabel('Standard Deviation')
title('Standard deviation of cracks size at a given time')
grid

disp('Run the program for the other inspection techniques and compare
the value of the optimization function and probability of failure to
obtain the optimum nondestructive inspection technique (NDI) and its
associated inspection interval')
```